Review

Oxidative desulfurization and denitrogenation of fuels using metal-organic framework-based/-derived catalysts

Biswa Nath Bhadra, Sung Hwa Jhung*

Department of Chemistry and Green-Nano Materials Research Center, Kyungpook National University, Daegu 41566, Republic of Korea

ABSTRACT

Removal of sulfur- and nitrogen-containing compounds (SCCs and NCCs) from commercial fuel is very important since those impurities can cause various problems including catalyst deactivation and acid rain. Because of the limitations of the conventional refinery methods, development of a new method such as oxidative desulfurization (ODS) is highly desirable. Metal-organic frameworks (MOFs)-based and MOF-derived nanohybrid materials were suggested as a good catalyst for ODS of fuels. Moreover, removal of NCCs via oxidation with MOF-derived catalyst was also reported even though the technique is just emerging. Therefore, it is required to analyze the reported results; and more importantly to suggest a new research direction; and finally, to estimate the possibility of new desulfurization/denitrogenation technology that might replace/compensate studied technologies. This review might be quite beneficial not only to accumulate or understand the reported results but also to develop new efficient catalysts for the probable commercialization of the ODS/ODN technology.

1. Introduction

Approximately 90% of the global energy resources have been originated from fossil fuels, and their demand or exploration is increasing with the current technological advancements and the increasing population worldwide [1]. Moreover, new and unconventional fuel resources are being explored to meet the increasing needs of energy [2,3]. These fossil fuels generally consist of a large number of impurities, and removal of those contaminants before the utilization is one of the supreme concerns in recent decades.

Among the wide variety of contaminants in fossil fuels (e.g. crude oil, jet fuel, furnace oil, gasoline, diesel, and etc.), naturally occurring sulfur- and nitrogen-containing organic compounds (SCCs and NCCs, respectively) are the major groups of the contaminants [4–6]. Sulfides, disulfides, mercaptans as well as thiophene (Th) and its derivatives (for example, as shown in Table 1, benzothiophene (BT), dibenzothiophenes (DBTs), 4-methylbenzothiophene (4-MBT), 4,6-dimethyldibenzothiophene (4,6-DMDBT), 3,7-dimethyldibenzothiophene (3,7-DMDBT), and 2,8-dimethyldibenzothiophene (2,8-DMDBT)) are common SCCs that exist in fuels. Moreover, generally, two kinds of NCCs such as basic (pyridine, quinoline (QUI), tetrahydroquinoline, acridines and aniline, and their derivatives) and non-basic or neutral (pyrrole (PRL), indole (IND), carbazole (CBZ), and their derivatives) ones are found in fossil fuels (Table 1). These types of SCCs and NCCs release toxic SO_x and

NO_x, respectively, upon combustion, and cause severe health/environmental problems, including air and water pollution, global warming, ecological instability, and acid rain as well as the harmful impact on living organisms [6–9]. SCCs and NCCs are also responsible for catalyst poisoning as well as rust refinery equipment in fuel processing technologies. To protect the environment as well as fuel processing technology, the European Union (E.U.) legislation and U.S. Environmental Protection Agency (EPA) set the maximum allowable S-content of 10 ppmw and 15 ppmw, respectively [6,10,11]. On the other hand, contaminants based on NCCs require more attention because of their high contents in fossil fuels [12] and chemically active characteristics. These NCCs not only deactivate the catalyst efficiency in hydrodroprecessing process (HD-process; the established industrial method for desulfurization/denitrogenation) but also rust refinery equipment and block pipelines in fuel processing technology [13–15]. Consequently, removal of NCCs is the first priority before carrying out the desulfurization. Therefore, worldwide researchers have investigated to find an effective method to remove these harmful compounds (SCCs and NCCs) from crude oils for effective utilization [10,11].

Thus far, a number of methods including hydro-desulfurization/-denitrogenation (HDS/HDN) [10,16–20], bio-desulfurization/-denitrogenation [21,22], extractive desulfurization/denitrogenation (EDS/EDN) [23–25], adsorptive desulfurization/denitrogenation (ADS/AND) [15,20,26–29] and oxidative desulfurization/denirtogenation (ODS/
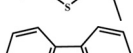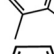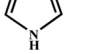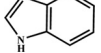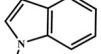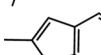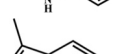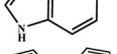
Table 1
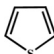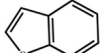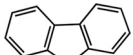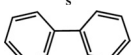Molecular dimension and electron density of the studied SCCs and NCCs.

SCCs and NCCs	Chemical structure	Molecular dimension [29]	Electron density on S [31] or N [50] atom for SCCs and NCCs, respectively (e/bohr^3)
Thiophene (Th)		4.79 Å × 5.26 Å	5.696
Benzothiophene (BT)		5.63 Å × 7.43 Å	5.739
Dibenzothiophene (DBT)		6.07 Å × 9.81 Å	5.758
4-methyldibenzothiophene (4MDBT)		6.01 Å × 9.82 Å	5.759
2,6-dimethyldibenzothiophene (2,6-DMDBT)		6.26 Å × 9.8 Å	5.760
Pyrrole (PRL)			7.465
Indole (IND)			7.596
1Me-Indole (1Me-IND			7.471
2Me-Indole (2Me-IND)			7.591
3Me-Indole (3Me-IND)			7.566
Carbazole (CBZ)			7.650
Quinoline (QUI)			7.423

ODN) [20,30–35] have been developed and tried for the removal of NCCs and SCCs. Among the studied techniques, ODS might be one of the most promising methods for desulfurization because of its advantages like mild and simple processing as well as the high efficiency in removing stubborn aromatic thiophenes including Th, BT, DBT and 4,6-DMDBT [31–40]. Compared with ODS, ODN was studied scarcely or only a few studies devoted to the ODN [41–50]. For studying ODS or ODN, finding efficient catalysts is highly desirable. A number of catalysts based on W, Mo, V, Cu, Cu, and Ti and metals (such as polyoxometalates and their nanocomposites [36,37,51], WO$_x$-supported ZrO$_2$ [40,52], tungsten nitride/porous carbon [53], Co nanoparticle/porous carbon [54], monoclinic VO$_2$ [55], V$_2$O$_5$/Al$_2$O$_3$ [56], TiO$_2$/porous glass [57], titanium silicalite (TS-1) [58], titanate nanotubes [59], MoO$_x$ [60,61] and Cu nanoparticle anchored graphitic boron nitride [62]) have been developed as efficient ODS catalysts. Moreover, metal-free catalysts such as nitrides and reduced graphene oxide were also developed for ODS [63–66]. However, again, studies on ODN is in a very primitive stage.

Recently, metal-organic frameworks (MOFs) that are constructed of metal nodes coordinated with organic ligands (where the metal sites are uniformly dispersed throughout the frameworks) have attracted much attention for various potential applications owing to their high porosity, designable pore structure, and ready modification/functionalization [15,26,27,67–87]. In addition, interests on MOFs were boosted up for their capability to act as a unique precursor for generating highly porous carbon-based-nanomaterials via carbonization [87–98]. MOFs

including pristine and modified ones along with MOF-derived nanomaterials were found as efficient heterogeneous catalysts [99–102]. To date, there are several reports on the plausible ODS using MOF-based or MOF-derived catalysts with remarkable efficiency. However, to the best of our knowledge, there is no review article on ODS or ODN with MOF-based or MOF-derived materials even though there were some review papers on ADS/ADN [15,26,27,103]. In this review, we focus on the current developments of MOF-based and MOF-derived catalysts mainly for ODS of fuel (as shown in Fig. 1). Not only the summary on the reported results but also prospects in the field will be presented.

2. Oxidative desulfurization

2.1. Oxidative desulfurization over pristine MOFs

Several MOFs composed of transition metals including Ti, V, Zr, Co and Cr (structures of typical MOFs are illustrated in Fig. 2a-e) showed their activity in the ODS or in the oxidative removal of SCCs from model fuels. This section includes a brief summary (Table 2) of the efficiency and influential factors for ODS over the pristine MOFs without defects.

MOFs composed of Ti-metal (pristine MIL-125-Ti and its amine-functionalized analogue, NH$_2$-MIL-125-Ti, structure of the MIL-125-Ti is shown in Fig. 2a) were applied for the ODS of DBT with an oxidant of cumene-hydroperoxide (CHP) [104]. The results showed that MIL-125-Ti (conversion: 36%) was much efficient than the NH$_2$-MIL-125-Ti (conversion: 9%) in a reaction at 80 °C. On the other hand, the
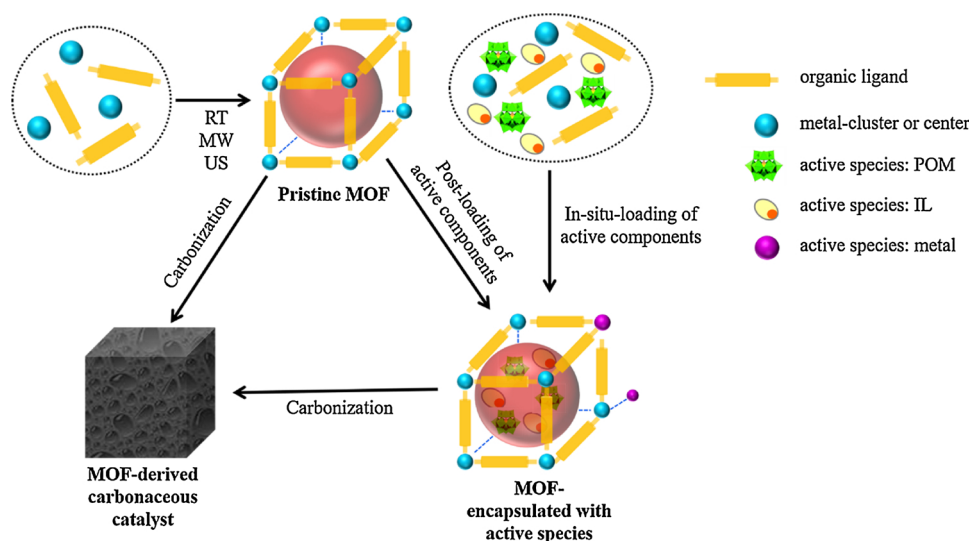
Fig. 1. Overview of the MOF-based and MOF-derived catalysts for ODS/ODN.

(a) MIL-125-Ti
12.55 and 6.13 Å, and 5–7 Å

(b) MIL-47-V
10.5 Å × 11 Å

(c) Ti-BDC
micropore / mesopore

(d) TMU-12

(e) H$_2$N-TMU-53

(f) MIL-101-Cr
29 and 34 Å, and 12 and 16 Å

(g) UiO-66-Zr
10.2 and 6.0 Å

(h) UiO-67-Zr
14.4 and 8.3 Å

(i) NU-1000-Zr
30.0 Å

(j) MOF-808-Zr
18.4 and 10.0 Å

(k) MIL-100-Fe
29 and 25 Å, and 8.6 and 5.8 Å

(l) ZIF-8-Zn
12.0 Å and 3.4 Å

(m) IRMOF-3-Zn
12.9 Å (from PSD)

(n) Keggin type HPA
~ 13–14 Å

Fig. 2. The crystal structures and pore or window size of the MOFs including (a) MIL-125-Ti, (b) MIL-47-V, (c) Ti-BDC, (d) TMU-12-Co, (e) H$_2$N-TMU-53-Co, (f) MIL-101-Cr, (g) UiO-66-Zr, (h) UiO-67-Zr, (i) NU-1000-Zr, (j) MOF-808-Zr, (k) MIL-100-Fe, (l) ZIF-8-Zn and (m) IRMOF-3-Zn, and (n) Keggin type HPA that dealt for studying ODS.

Table 2

Summary of the studies on the oxidative desulfurization over MOFs (pristine and defected ones). The reaction parameters including the studied SCCs, oxidant, initial concentration of SCCs, catalyst dosage, oxygen-over-sulfur ration, reaction temperature, reaction time, conversion, kinetic constant and activation energy, and remarks (as footnotes) are shown in the Table.

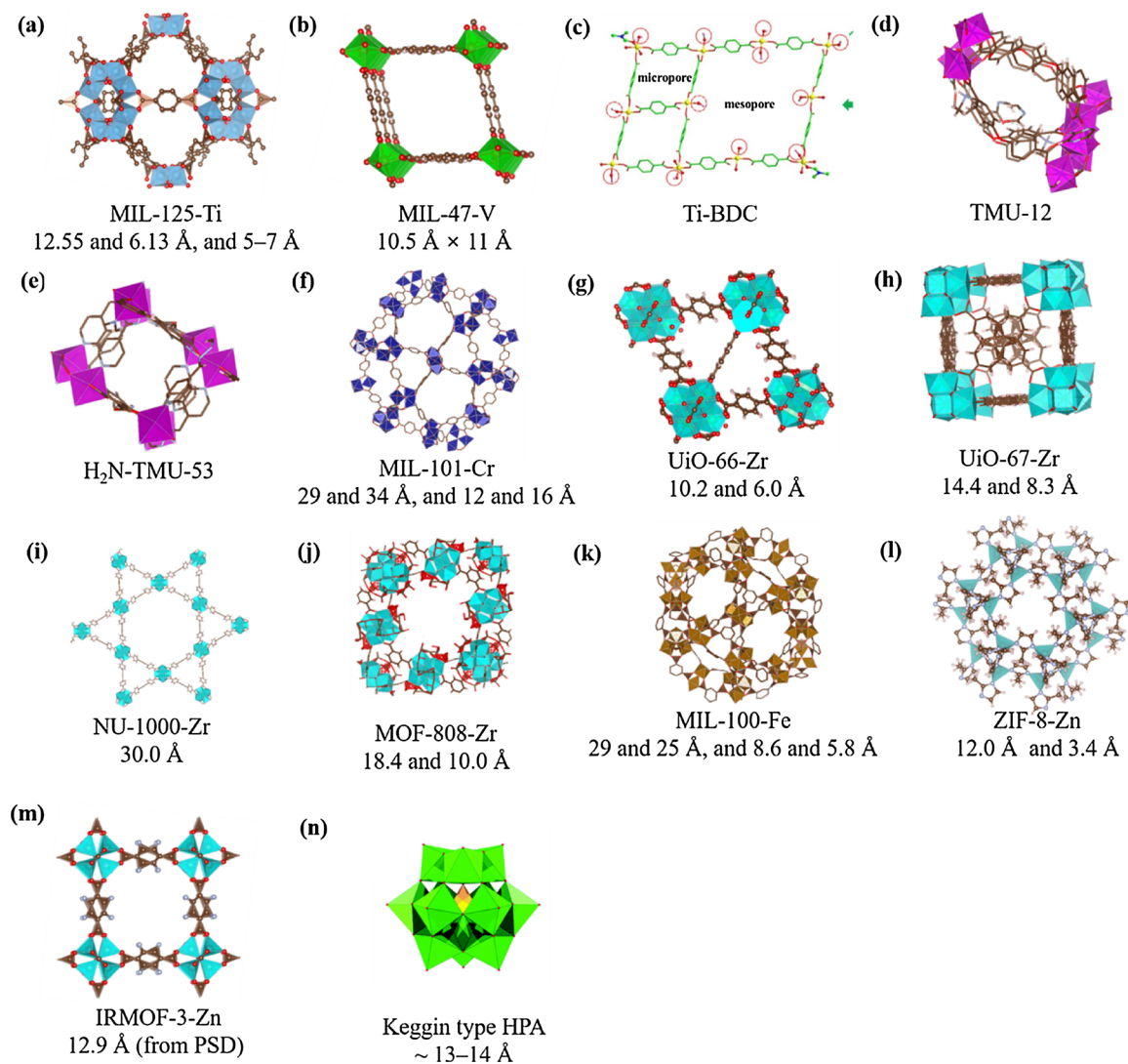| Catalysts	SCC	Oxidant	Conc. of SCC (ppm)	Catalyst amount (g/L)	O/S ratio	Reaction temperature (°C)	Reaction time (min.)	Conversion (%)	Kinetic constant (min^{-1})	Activation energy (KJ·mol^{-1})	Ref.
MIL-125-Ti	DBT	CHP	200	1.79	15	80	180	36	–	–	[104][a]
	4-MDBT							15			
	4,6-DMDBT							12		–	
NH$_2$MIL-125-Ti	DBT	CHP	200	1.79	15	80	180	9	–		
MIL-47-V	Th	TBHP	7165	0.64	2.15	80	180		1.3×10^{-3}	51	[106][b]
	BT		11428						9.9×10^{-3}		
	DBT		15691						2.9×10^{-2}		
MIL-125-Ti	Th	TBHP	7165	0.79	2.15	80			1.0×10^{-2}	75	[109][c]
	BT		11428						7.2×10^{-4}		
	DBT		15691						6.0×10^{-4}		
solv-micro-MIL-125-Ti	DBT	TBHP	1570	0.65	10	80			1.2×10^{-2}		
VAC-micro-MIL-125	DBT	TBHP	1570	0.65	10	80			1.2×10^{-2}		
meso-MIL-125-Ti	DBT	TBHP	1570	0.65	10	80			3.0×10^{-2}		
MIL-125-Ti(L)	Th	H$_2$O$_2$	170	0.1	8	60	240	70	–	–	[111][d]
	BT							91			
	DBT							100			
	4,6-DMDBT							60			
NH$_2$MIL-125-Ti	Th	H$_2$O$_2$	170	0.1	8	60	240	68	–	–	
	BT							84			
	DBT							98			
	4,6-DMDBT							59			
Ti-BDC-180	BT	H$_2$O$_2$	1000	3.52	6	60	45	92.3			[112][e]
	DBT							98.9			
	4,6-DMDBT							99.6			
TMU-10-Co	DBT	TBHP	500	4	12	60	120 and 480	19.8 and 40.2			[113][f]
TMU-12-Co	DBT	TBHP	500	4	12	60	120 and 480	35.5 and 75.2		13.4	
TMU-53-Co	DBT	H$_2$O$_2$	500	5	3	60	120	7.1			
H$_2$N-TMU-53-Co	DBT	H$_2$O$_2$	500	5	3	60	120	44.7	1.1×10^{-2}	15.57	[114][g]
NH$_2$-TMU-17-Zn	DBT	H$_2$O$_2$	500	5	3	60	120	37.1			
MIL-101(Cr)	DBT	O$_2$ of Air	200	0.5	5	120	1320	99.6			[115][h]
UiO-66-Zr	DBT	H$_2$O$_2$	1000	7.8	5	50	5	8.8			[117][i]
UiO-67-Zr	DBT	H$_2$O$_2$	1000	7.8	5	50	5	20.8			
NU-1000-Zr	DBT	H$_2$O$_2$	1000	7.8	5	50	5	11.1			
MOF-808-Zr	DBT	H$_2$O$_2$	1000	7.8	5	50	5	~100		22.0	
UiO-66-Zr(H)	DBT	H$_2$O$_2$	1000	5.0	6.0	60	120	5.6			[119][j]
Ti-UiO-66-Zr(H)	DBT	H$_2$O$_2$	1000	5.0	6.0	60	120	66.3			
Ti-UiO-66-Zr(D)	BT	H$_2$O$_2$	1000	5.0	6.0	60	120	50.7			
Ti-UiO-66-Zr(D)	DBT	H$_2$O$_2$	500	5.0	6.0	60	120	80.1			
UiO-66-Zr	4,6-DMDBT	H$_2$O$_2$	500	20		50	30 and 60	91.7			[120][k]
	DBT		1000					66.2			
	4-MDBT							98 and 99			
	4,6-DMDBT										
UiO-66-Zr$_{mod}$	DBT	H$_2$O$_2$	500	20		50	30 and 60	72 and 96.5			
UiO-66-Zr$_{HClmod}$	DBT	H$_2$O$_2$	500	20		50	30 and 60	60 and 85			
UiO-66-Zr$_{HCl}$	DBT	H$_2$O$_2$	500	20		50	30 and 60	38 and 40			
UiO-66-Zr$_{solvent}$	4,6-DMDBT	H$_2$O$_2$	1000	5.0	6.0	60	120	80.5			[121][l]
	DBT		500					52.5			
UiO-66-Zr$_{free}$	DBT	H$_2$O$_2$	1000	5.0	6.0	60	120	99.6			
	4,6-DMDBT		500					98.1			
UiO-66-Zr$_{0.5h}$	DBT	H$_2$O$_2$	1000	2.5	59	60	60	~98			[122][m]

4

Table 2 (continued)

Catalysts	SCC	Oxidant	Conc. of SCC (ppm)	Catalyst amount (g/L)	O/S ratio	Reaction temperature (°C)	Reaction time (min.)	Conversion (%)	Kinetic constant (min⁻¹)	Activation energy (KJ·mol⁻¹)	Ref.
UiO-66-Zr$_{1.0}$	DBT	H$_2$O$_2$	1000	2.5	59	60	60	~98			
UiO-66-Zr$_{10h}$	DBT	H$_2$O$_2$	1000	2.5	59	60	60	~85			
UiO-66-Zr$_{20h}$	DBT	H$_2$O$_2$	1000	2.5	59	60	60	~18			
UiO-66-Zr	Th	H$_2$O$_2$	500	10	12	60	150	49		57	[124]ⁿ
	BT							58			
	DBT							100			
	4,6-DMDBT							67			

[a] Pore size effect; less steric hindrance to the defected Ti-O active sites, higher the activity.
[b] V^{iv} center is more active than Ti^{iv}; however, MIL-47-V was less stable than MIL-125-Ti.
[c] Hierarchically mesoporous MIL-125-Ti leads to exposure of additional active sites resulting in higher catalytic activities.
[d] Different from common catalysis, catalysts with larger particle size showed better performance than the smaller ones due to higher number of unsaturated Ti^{IV}-sites.
[e] Rich mesoporosity and active Ti-OH sites influenced the higher performance.
[f] Coordination environment of Co centers and void space lead higher activity of TMU-12-Co.
[g] Basic − NH$_2$ group may have the influential role on ODS performance.
[h] Peroxo and superoxo species generated by molecular oxygen by the MIL-101-Cr that influenced the catalysis.
[i] Coordination environment and density of active Zr-OH species played an important role for higher efficiency of MOF-808-Zr.
[j] Catalytic performance might be mainly attributed to the introduction of active Ti^{IV}-sites, although Zr-sites of UiO-66-Zr also can oxidize SCCs.
[k] Higher the defect, higher the ODS performance.
[l] Increased defect sites via solvent-free synthesis of the MOF boosted the ODS performances.
[m] Defect sites, that influenced the ODS performance, can be tuned by changing synthesis time.
[n] Lewis-acid side of the MOF created active oxygen species that influenced the ODS of SCCs.

conventional Ti-catalysts, micro-TS-1 and meso-TS-1, showed the conversion of 6% and 97%, respectively, under the very same conditions (Fig. 3a). These results suggested that titanium species in a tetrahedral (rather than octahedral) coordination (Ti^{IV}) are the primary active sites for ODS reactions [105]. Moreover, the molecular dimension of SCCs and pore or window size of the catalyst played the most vital role in the ODS reactions. For instance, the order of activity (MIL-125-Ti > H$_2$N-MIL-125-Ti > micro-TS-1) for DBT conversion follows the order of their pore/window sizes of MOFs (6.1 Å, 5.9 Å and 5.6 Å × 5.3 Å for MIL-125-Ti, H$_2$N-MIL-125-Ti and micro-TS-1, respectively). Consequently, DBT cannot access the titanium sites located inside the pores of MIL-125-Ti, H$_2$N-MIL-125-Ti and micro-TS-1; thereby, the activity was very low; whereas, meso-TS-1 composed of mesopores (up to ˜20 nm of maximum pore width, which is easily accessible for DBT) with active titanium species showed high conversion because of ready diffusion of bulky DBT (6.07 Å × 9.81 Å [29]). On the other hand, the oxidation (even low conversion) of DBT over the MIL-125-Ti and H$_2$N-MIL-125-Ti could be explained with defected Ti-O sites (present mainly outside of the pores) that can activate the oxidant CHP. The lower conversion of 4-MDBT (˜15%) and 4,6-DMDBT (˜12%) (compared with that of DBT, 36%) over the MIL-125-Ti (Fig. 3b) again showed the importance of pore-size and the molecular dimension of reactant in the oxidation reactions.

A more detailed study on the ODS of fuel was conducted using MIL-47-V (a V-based MOF) and MIL-125-Ti in the presence of tert-butyl hydroperoxide (TBHP) as an oxidant [106]. The results demonstrated that MIL-47-V was superior, both in terms of pseudo-first-order rate constant and activation energy (E_a), to the MIL-125-Ti in the catalytic oxidation of DBT. The reactivities increased consistently with increasing the reaction temperature for both of the MOFs; however, the relative apparent rate constants of the studied MOFs varied with the reaction temperature. For example, the MIL-47-V showed 32-, 48- and 88-times larger rate constants to that of MIL-125-Ti at 100 °C, 80 °C, and 60 °C, respectively. Importantly, the MIL-47-V showed much faster reaction rates than MIL-125-Ti in the oxidation of DBT, especially at low temperature (60 °C). MIL-125-Ti is composed of triangular windows sizes in the range of 5–7 Å (even with two types of cages (12.55 and 6.13 Å, Fig. 2a) with octahedral and tetrahedral Ti-species [107]) which are not large enough for DBT (6.07 Å × 9.81 Å [29])) to diffuse into the pores of MIL-125-Ti. However, MIL-47-V with octahedral V-species [108] has a large pore, with a dimension of 10.5 Å × 11 Å (Fig. 2b), which is large enough for DBT to access to the active metal center inside the pores. For the same reason, BT (5.63 Å × 7.43 Å [29]) was oxidized with higher kinetics over the MIL-47-V (9.9 × 10^{-3} min^{-1}) than over the MIL-125-Ti (1.0 × 10^{-4} min^{-1}). Consequently, it was suggested that the insufficient accessible pore size might be the main reason for low activity of MIL-125-Ti in the oxidation of DBT even composed of tetrahedral Ti-species. Small reactivity of MIL-125-Ti could be explained with four coordinated Ti-species (located on the outer surface) that behaved as active sites for oxidation reactions. The assumption was confirmed further from the small differences in the activity for Th (a smaller SCC with a molecular dimension of 4.79 Å × 5.26 Å) [29]. For instance, MIL-47-V (1.4 × 10^{-3} min^{-1}) had only twice faster kinetics to that of the MIL-125-Ti (7.0 × 10^{-4} min^{-1}) under the reactions at 80 °C. In addition, investigations on the stability (via XRD analysis) of the MIL-47-V structures indicated the degradation of MIL-47-V after the treatment in the presence of TBHP (without DBT) in decane solution. The XRD and XPS analyses revealed the formation of BDC, V^{5+} and V^{3+} species upon breaking of the MIL-47-V; however, interestingly, remain intact (nearly) after the ODS reaction of DBT. These observations suggested that the reactant molecules (DBT) themselves sheltered to keep the structural integrity and chemical property or slowed the degradation rate via preventing probable over-oxidation of MIL-47-V by TBHP. This might be meaningful considering industrial applications of the material. However, MIL-125-Ti appeared stable in the presence of TBHP even under harsh reaction conditions (24 h at 100 °C). These results
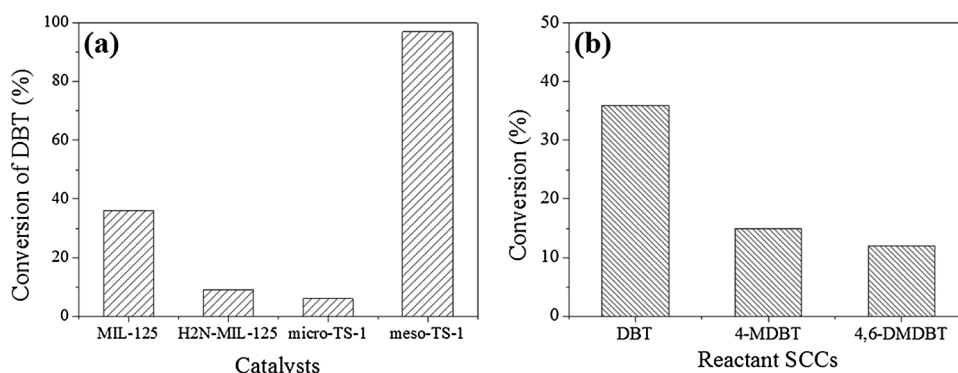
Fig. 3. (a) Conversion of DBT over MIL-125-Ti, NH$_2$-MIL-125-Ti, micro-TS-1 and Meso-TS-1, and (b) conversion of DBT, 4-MDBT and 4,6-DMDBT over the MIL-125-Ti (Reproduced from Ref. [104], Copyright 2013 Elsevier).

suggested that the V metal centers in MIL-47-V seemed to have a higher activity (however, lower stability) than the Ti centers in MIL-125-Ti in the oxidative removal of SCCs from fuel [106].

Considering the lower activity of microporous MIL-125-Ti, McNamara and Hicks et al. [109] developed a new method to synthesize hierarchically porous MIL-125-Ti to improve the catalytic activity of the MOF. Mesoporous MIL-125-Ti was synthesized via vapor-assisted crystallization method (Fig. 4a) in the presence of cetyltrimethylammonium bromide (CTAB) as a surfactant. To determine the benefits of mesoporosity, oxidations of DBT were conducted at 80 °C over the meso-MIL-125-Ti along with two other microporous MIL-125-Ti MOFs (solv-micro-MIL-125-Ti and VAC-micro-MIL-125-Ti, that were synthesized via conventional solvothermal and vapor-assisted crystallization method, respectively). The results, as illustrated in Fig. 4b and Table 2, revealed that the activity of both the solv-micro-MIL-125-Ti and VAC-micro-MIL-125-Ti samples exhibited a similar rate constant ($k_{app} = 1.2 \times 10^{-2}$ min^{-1} and 1.2×10^{-2} min^{-1}, respectively), which was also in accordance with the similar surface areas of the catalysts. However, the meso-MIL-125-Ti displayed significantly improved (about twice faster) activity ($k_{app} = 2.3 \times 10^{-2}$ min^{-1}) than the microporous samples even with a lower surface area. Additionally, the meso-MIL-125-Ti material was not only superior to microporous MIL-125 s in its catalytic activity but also found as stable upon subsequent regeneration after three recycles. The improved performance was simply originated from the introduction of mesoporosity rather than the formation of different active sites.

Inspired by the studies on the oxidation of alkylphenols to p-benzoquinones catalyzed by MIL-125-Ti via activation of H$_2$O$_2$ [110], Yang et al. [111] studied the ODS of a series of SCCs over MIL-125-Ti by replacing the oil-soluble oxidant (e. g. CHP and TBHP) with an oil-insoluble oxidant (H$_2$O$_2$) in the presence of additional extractant methanol. The biphasic catalytic oxidation of SCCs over a few MIL-125-Ti MOFs with different crystal sizes and NH$_2$-MIL-125-Ti in the presence of H$_2$O$_2$ could show highly improved removal efficiency for the studied SCCs. Different from inferior catalytic performance of catalysts with larger particles (that observed in common), here, large-sized MIL-125-Ti (MIL-125-Ti(L), (7–8 μm) outperformed medium-sized MIL-125-Ti (M) (1–3.2 μm), small-sized MIL-125-Ti(S) (0.7–1.6 μm) and small-sized NH$_2$-MIL-125-Ti (0.18–0.45 μm) in oxidation of SCCs. However, the oil-soluble oxidant TBHP cannot oxidize the DBT in the presence of MeOH (the extractant). In addition, the observed low stability of MIL-125-Ti (L) in the oxidation in the presence of water (instead of methanol extractant) suggested that MeOH not only extracted oxidation products but also played a vital role in protecting the structure of MIL-125-Ti(L). The notably enhanced catalytic activity of MIL-125-Ti(L) in ODS in the presence of water was explained by the authors with the much unsaturated tetrahedrally coordinated Ti^{IV} species; however, further study might be required to understand the unusual results. Ye et al. [112] also showed the importance of unsaturated tetrahedral Ti^{IV} in the ODS of

SCCs using mesoporous Ti-BDC with much coordinatively unsaturated Ti^{IV} sites. Hierarchically porous Ti-BDC-180 (amorphous material, prepared at 180 °C) showed very good efficacy after 45 min at 60 °C in the removal of BT (92.3%), DBT (98.9%) and 4,6-DMDBT (99.6%) from N-O ctane via oxidation with H$_2$O$_2$ (as an oxidant) in the presence of acetonitrile (MeCN; as an extractant). However, unfortunately, there was little discussion on the reason for high efficiency and evidence of the presence of unsaturated tetrahedral Ti^{IV} in the studied catalyst was not provided in detail.

Along with Ti- and V-based MOFs, Co-based MOFs [Co$_6$(oba)$_5$(OH)$_2$(H$_2$O)$_2$(DMF)$_4$]$_n$·5DMF (TMU-10-Co) and [Co$_3$(oba)$_3$(O) (Py)$_{0.5}$]$_n$·4DMF·Py (TMU-12-Co) (oba = 4,4′-oxybisbenzoate and Py = pyrazine) also showed good catalytic activity and reusability in ODS reaction of model oil (DBT in n-hexane) in the presence of TBHP [113]. Among the two Co-MOFs, TMU-12-Co (Fig. 2d) showed better performance than the TMU-10-Co in the oxidation of DBT for the whole range of tested reaction times. For example, TMU-10-Co showed 19.8% conversion after 2 h which increased up to 40.2% in 8 h; however, TMU-12-Co displayed a quite high conversion (75.2%) after 8 h which was 35.5% in 2 h. The different performances of TMU-10-Co and TMU-12-Co in the oxidation of DBT are possibly because of a difference in their coordination environment of Co centers (e.g. regular and distorted octahedral Co-species for TMU-10-Co and TMU-12-Co, respectively) and void space (32.7% and 43% of TMU-10-Co and TMU-12-Co, respectively). Very recently, Abazari et al. [114] reported another Co-MOF (H$_2$N-TMU-53-Co (Fig. 2e) or [Co(2-ATA)$_2$(4-bpdb)$_4$]$_n$ (2-ATA: 2-aminoterephthalic acid and 4-bpdb: N,N-bis-pyridin-4-yl-methylene-hydrazine)) was active in ODS reaction in the presence of H$_2$O$_2$ (as an oxidant). After 4 h of reaction at 50 °C, the S-content (DBT) reduced to 96 ppm from 500 ppm (~80% removal, where 34.8% was contributed by the adsorption) using H$_2$N-TMU-53-Co as a catalyst. Moreover, two NH$_2$ functionalized MOFs with different metal centers (H$_2$N-TMU-53-Co and NH$_2$-TMU-17-Zn; MOFs composed of Co and Zn, respectively) showed comparable DBT conversion after 1 h (or, NH$_2$-TMU-17-Zn and H$_2$N-TMU-53-Co showed ~ 37% and ~ 45%, respectively). However, the ODS efficiency of TMU-53-Co without -NH$_2$ functionality was much lower (7.1% DBT conversion) than the H$_2$N-TMU-53-Co. These results indicated the -NH$_2$ functionality, rather than the metal center of the studied MOFs, was important in the ODS reactions. Further study might be required since there was little detailed explanation on the contribution of the amino group in the ODS. Curiously, the ODS over TMU-12-Co and H$_2$N-TMU-53-Co showed very low activation energy (E_a = 13.4 and 15.57 kJ/mol, respectively) [114]; however, there is a possibility that this activation energy might be related to DBT diffusion (to the active sites of porous MOFs in liquid phase) of substrate rather than the catalysis or oxidation of DBT. Or, further work is required to confirm the ODS under without diffusion limitation.

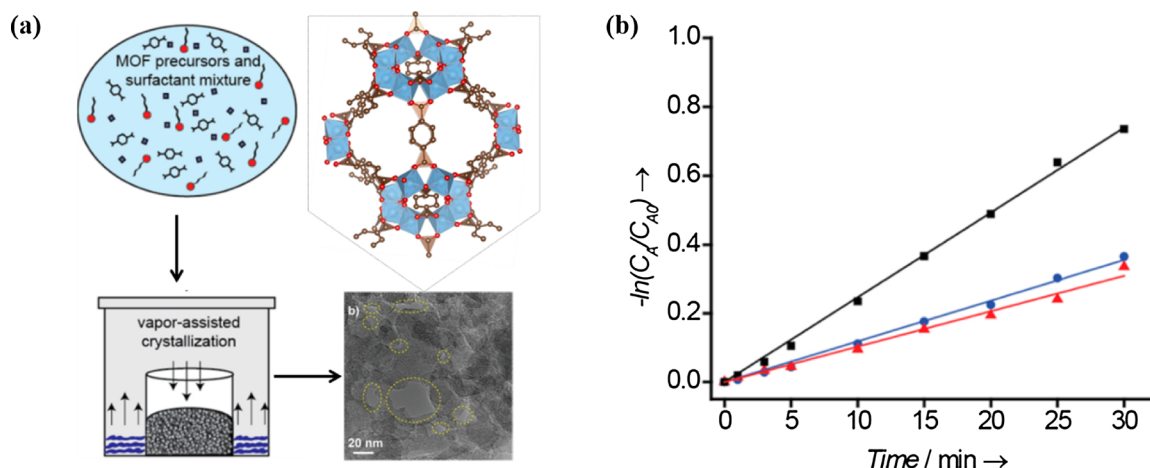Very interestingly, MIL-101 (Fig. 2f; pore diameters of 29 and 34 Å

(a)

(b)

Fig. 4. (a) Schematic representation of the synthesis of hierarchically microporous/mesoporous MIL-125-Ti via the vapor-assisted crystallization method, and (b) pseudo-first-order kinetic plots that generated via curve fitting of the oxidation of DBT in model fuel. Here, blue •, red ▲, and black ■ represented the plots for solv-micro-MIL-125-Ti, VAC-micro-MIL-125-Ti, and meso-MIL-125-Ti, respectively (Adapted from Ref. [109], Copyright 2015 ACS).

with windows of 12 and 16 Å), highly porous MOFs with Cr or Fe metal center showed promising desulfurization efficiency (up to ˜5.3 ppm S) via aerobic oxidation of SCCs (200 ppm S) from fuel where water was used as extractant to remove oxidized sulfones rather than sulfoxides [115]. The ODS activity of MIL-101-Cr was said to be higher than the MIL-101-Fe even though the performance of two MIL-101 materials showed similar performances. The oxidation efficiency over the MIL-101-Fe was highly dependent on the activation process (Fe^{3+} in MIL-101-Fe could be reduced to Fe^{2+} [116]); however, no influence was observed for the MIL-101-Cr. Moreover, the occurrence of a temporal induction period was observed when the reactions were conducted without any pre-activation treatment, which can be minimized by pre-activation of the MOF. No initial induction period was observed for all of the three pre-activated reaction media (as shown in Fig. 5), which indicated the role of diffusion of n-dodecane rather than the diffusion of DBT or oxygen into the MIL-101-Cr pores. Even though these results can be confirmed from the observed higher oxidation efficiency of DBT in the n-alkane having shorter chain length compared to that of n-alkanes having a longer chain, more detailed studies might be required. Moreover, increasing oxygen pressure and reaction temperature can reduce the induction period even though the reaction rate was not affected. Therefore, it can be suggested that the ODS can be conducted with MIL-101-Cr catalyst under air (instead of using any peroxides). Even though the ODS with the MOF showed a very high E_a value (137 kJ·mol^{-1}), the catalyst had very good recyclability.

Zhang et al. [117] demonstrated that conventional UiO-66-Zr (highly crystalline, without defect) had high initial activity in the oxidation of SCCs at 60 °C in the presence of H_2O_2 and MeOH (as an oxidant and extractant, respectively). The authors assumed that efficient ODS reaction was because of Lewis acid sites (from unsaturated Zr^{IV} species) of non-defected UiO-66-Zr. However, unsaturated Zr^{IV} sites might be unusual with perfect UiO-66-Zr crystals; therefore, further works are required to confirm the idea of Lewis acid sites on defect-free UiO-66. On the other hand, the MOF had poor recyclability, which was explained by the incomplete removal of the strongly adsorbed sulfones (that produced upon the oxidation of SCCs) on the active sites of UIO-66-Zr catalyst. Moreover, a recent study demonstrated, as shown in Fig. 6, the ODS performances of a series of Zr-based MOFs (UiO-66-Zr (Fig. 2g), UiO-67-Zr (Fig. 2h), NU-1000-Zr (Fig. 2i) and MOF-808-Zr (Fig. 2j)) [118] in the presence of H_2O_2 (as an oxidant) and MeCN (as an extractant) at 50 °C. Among the tested Zr-MOFs, MOF-808-Zr showed a remarkable efficacy (˜100% conversion of 1000 ppm DBT) in ODS of DBT within 5 min at 40 °C (Fig. 6b), with very good recyclability (Fig. 6c). Notably, MOF-808-Zr exhibited very low activation energy (22.0 KJ·mol^{-1}) and high TOF value (42.7 h^{-1}), which was also

capable to oxidize BT (16.7% conversion) and 4,6-DMDBT (94.7%) (Fig. 6d). The six connected Zr_6 cluster along with a higher number of active Zr-OH sites might be responsible for the higher activity of MOF-808-Zr than the defect-free UiO-66-Zr (12 connected), UiO-67-Zr (12 connected), and NU-1000-Zr (8 connected). In addition, the efficiency of Ti-functionalized defect-free UiO-66-Zr was evaluated for ODS of DBT and thioanisole from fuel [119], although the oxidation method and Ti incorporation strategy were different from an earlier study [120]. Here, they used TiO(acac)$_2$ in anhydrous MeOH to form active Zr-OTi^{iv} species via replacing hydrogen atom of the Zr-OH (rather than the replacing Zr metal of UiO-66-Zr with Ti metal), as illustrated in Fig. 7a. Ti-functionalized UiO-66-Zr showed insufficient removal of large DBT both in batch (up to 75 ppm from 1000 ppm) and continuous-flow (up to 276 ppm from 1000 ppm) oxidations, nevertheless the functionalized UiO-66-Zr showed better performance than the pristine UiO-66. Interestingly, thioanisole was removed completely from the oil phase within only eight minutes with the functionalized MOF. The complete or fast oxidation of thioanisole might be governed by the easy accessibility of small thioanisole molecule into UiO-66-Zr pore.

2.2. Oxidative desulfurization over defected MOFs

UiO-66 s, synthesized in various conditions, were applied in ODS, and physicochemical properties of the MOFs had a dominant role in the oxidation. Granadeiro et al. [121] studied the oxidative removal of DBT, 4-MDBT and 4,6-DMDBT from fuel in a biphasic system with acetonitrile and H_2O_2 (as extractant and oxidant, respectively) using four different UiO-66-Zr MOFs (UiO-66-Zr$_{mod}$, UiO-66-Zr$_{HCl}$, UiO-66-Zr$_{HCl\cdot mod}$, and UiO-66-Zr) that prepared with four different methods. Here, the subscripts mean the used crystallizing agent (HCl) and modulator (trifluoroacetic acid) where no crystallizing agent and modulator was used for UiO-66-Zr. As shown in Fig. 8, the oxidation results showed an activity order: UiO-66-Zr > UiO-66-Zr$_{mod}$ > UiO-66-Zr$_{HCl\cdot mod}$ > > UiO-66-Zr$_{HCl}$. The highest activity over the low crystalline (as judged by XRD), linker deficient or structurally modified UiO-66-Zr (without HCl or trifluoroacetic acid) was explained by the role of defect sites that possibly enhanced the level of the formation of active Zr^{IV}–peroxo species via interaction between H_2O_2 and the solid UiO-66-Zr. Because of the high activity and exceptional recycling ability of UiO-66-Zr with defect sites, it was suggested as a very stable and robust heterogeneous catalyst for ODS.

Inspired by the positive role of defect sites on the superior ODS, a few studies were accomplished to boost up the oxidation performance via increasing the defect sites in the MOFs [122,123]. A facile/green
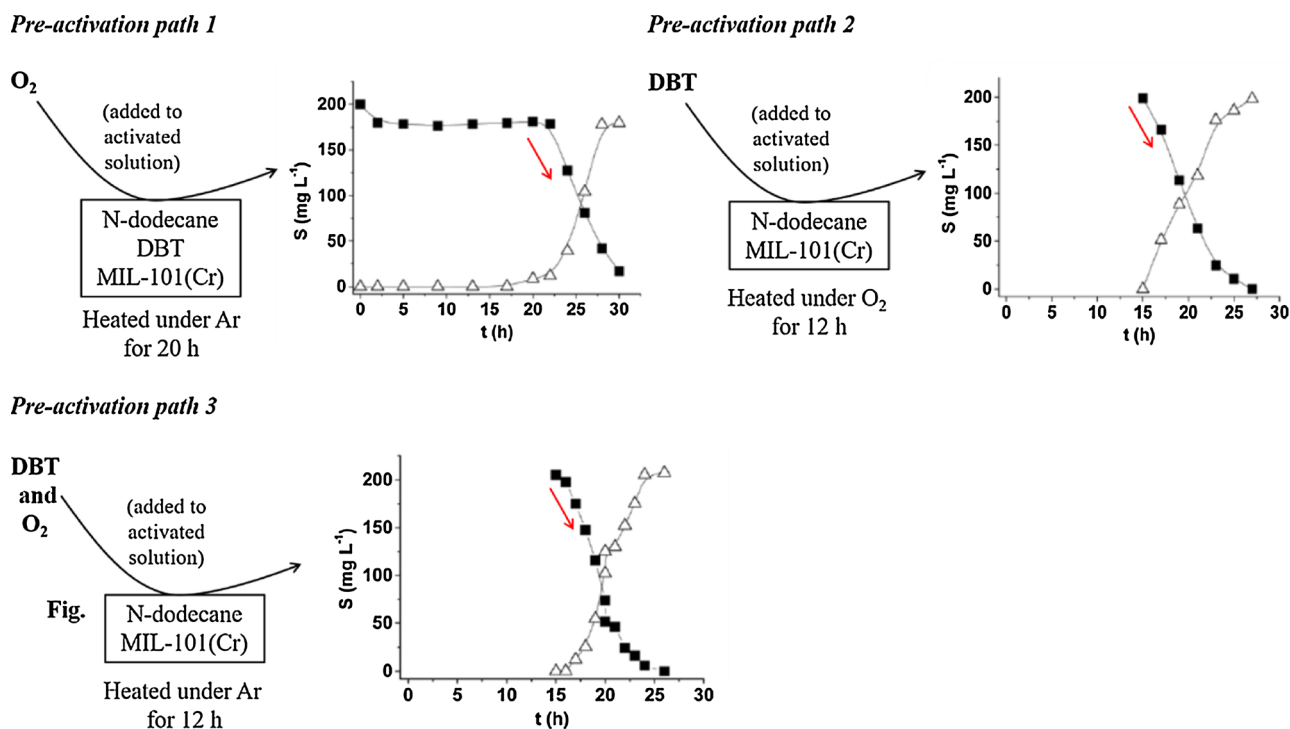
Fig. 5. Aerobic oxidation of DBT (■) to DBT-sulfone (△) using MIL-101(Cr) as a catalyst after the three different pre-activation paths; and the oxidation results were shown in the right side of each reaction condition (Reproduced from Ref. [115], Copyright 2016 Royel Society of Chemistry).

approach, namely solvent-free method (as illustrated in Fig. 9a), was developed for the synthesis of UiO-66-Zr (named as UiO-66-Zr$_{free}$) having a higher number (as estimated from Fig. 9b) of defect sites than the UiO-66-Zr$_{solvent}$ (as observed from Fig. 9c). The prepared UiO-66-Zr$_{free}$ showed (Fig. 9d) remarkable efficiency in the ODS of DBT and 4,6-DMDBT in the presence of H_2O_2, which was much higher than the UiO-66-Zr$_{solvent}$ (synthesized in DMF as solvent) and conventional UiO-66-Zr$_{HCl}$ (synthesized solvothermally in the presence of HCl). The higher activity again was governed by the higher defect sites (that originated from the higher number of missing linkers (2.16) per unit cell of UiO-66$_{free}$) that provided mainly the very active Zr-OH species. In addition, a facile method was adopted to create defect-sites in UiO-66-Zr via tuning the synthesis time, in which short time synthesis facilitates the formation of defects in UiO-66-Zr [123]. The UiO-66-Zr MOFs synthesized in 0.5 h and 1.0 h possess a high concentration of defects which showed excellent performance in the oxidation of DBT using H_2O_2 as oxidant. Again, Zr-OH species of the defected UiO-66-Zr was suggested as the active site for improved ODS activity.

Addition to the conventionally (single step) synthesized MOFs, metal-ion or ligand-exchanged MOFs were also used as catalysts for studying ODS [120,124]. For instance, Ti-exchanged UiO-66-Zr showed greatly enhanced (~11 fold) ODS performance compared to the highly crystalline parent UiO-66-Zr (without defect) [120]. This strategy (Fig. 7b) is efficient for both the conventional UiO-66-Zr and UiO-66-Zr with crystal defect. Again, the improvement might be attributed to the incorporation of active Ti^{iv} species in the UiO-66-Zr framework. Two other Zr-based MOFs (MOF-808-Zr) and {Zr$_6$O$_4$(OH)$_4$(C$_{24}$H$_{15}$(COO)$_3$)$_2$(HCOO)$_6$} (UMCM-309-Zr) were used as heterogeneous catalysts in ODS reactions [124]. These MOFs showed highly improved oxidation efficiency after the generation of a higher number of active Zr^{IV} open metal-sites via removal of the coordinated formate molecules by immerging the MOFs in MeOH. MOF-808-Zr (pristine or formate-free ones) showed better catalytic activity than the counterparts of UMCM-309-Zr, owing to its higher surface areas and pore volumes.

Since the high activity of UiO-66 for ODS was explained via defected [120–124] or defect-free MOFs [117], it will be required to check the

contribution of defects on ODS and analyze precisely concentration of defect sites of the studied MOFs to confirm the contribution of defects. Based on above, it can be summarized that MOFs composed of various metal centers including Ti, V, Co, Cr, and Zr might be very effective heterogeneous catalysts, in the presence of suitable oxidant, for oxidative removal of SCCs including Th, thioanisole, BT, DBT, 4-MDBT and 4,6-DMDBT from fuel under mild conditions. Along with the active metal component and pore/window size of the conventional MOFs, some of the synthesis and post-modification methods have influential roles in the effective oxidation of SCCs. Most of the MOFs are found to be quite stable and readily recyclable and thereby can be suggested as good catalysts for ODS, although some of them are not stable under the investigated conditions.

2.3. Oxidative desulfurization over active component-loaded MOFs

Various types of polyoxometalates (POMs) or heteropolyacids (HPAs) and ionic liquids (ILs) themselves along with their composites/derivatives were found to be effective catalysts for ODS [31,36,37,125–129]. However, it is noteworthy that the POM or HPA-based catalysts generally were non-porous and highly soluble excluding very special cases [130] and, therefore, difficult in reuse. Moreover, ionic liquids-based catalysts required relatively long processing time owing to low reactivity and complex recovery method, although the oxidations could be accomplished under moderate conditions and ILs were reusable without loss of activity. Therefore, POMs/HPAs or ILs, when supported suitably/firmly onto a porous material, could be applied effectively in ODS with ready recyclization. MOFs were also used as a porous support or host framework to encapsulate active POMs/HPAs or ILs [26,131–139], because of their well-defined structure with huge porosity, to develop better ODS catalysts. This section summarized (Table 3) the reported studies on the ODS over the POMs/HPAs or ILs-encapsulated MOFs including their preparation methods.

MIL-101-Cr was found to be an ideal MOF to encapsulate POMs (13–14 Å diameters) because of having the very high surface area and large pore sizes (29 and 34 Å) [140] along with its high hydrothermal
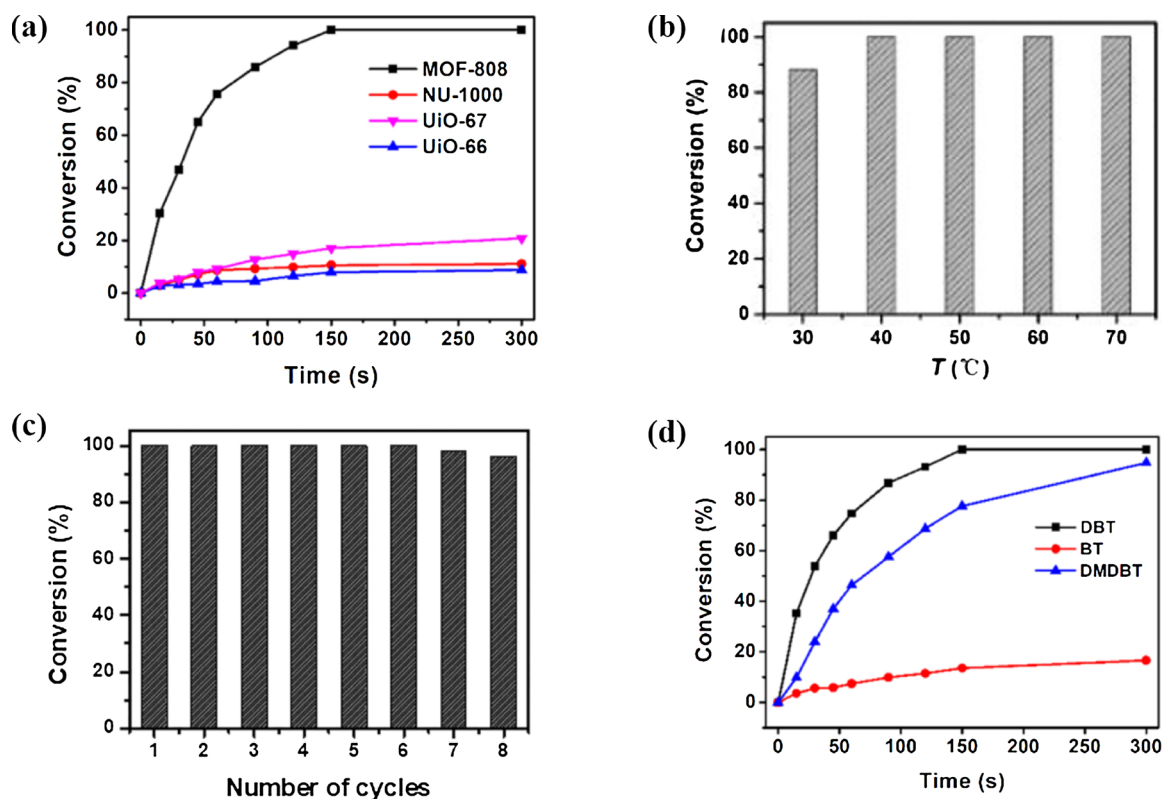
Fig. 6. (a) Conversion of DBT catalyzed by a series of Zr-MOFs (UiO-66-Zr, UiO-67-Zr, MOF-808-Zr, and NU-1000-Zr) (b) effects of temperature, (c) recycling experiments of MOF-808 catalyst for DBT oxidation and (d) oxidation of selected SCCs over MOF-808 under optimal reaction conditions (Adapted from Ref. [118], Copyright 2019 ACS).

and chemical stabilities. The structure of MIL-101-Cr (with pore dimensions) and a POM are illustrated in Fig. 2f and n. The POM/HPA-encapsulated MIL-101-Cr showed promising performance in various catalytic reactions. Therefore, several research groups studied the incorporation of various POMs/HPAs into MIL-101-Cr by different

techniques (Figs. 10–13), and the resulting POM/HPA@MIL-101-Cr catalysts were used in deep desulfurization of fuel via oxidation reaction in the presence of an oxidant. For example, Hu et al. [141] prepared phosphotungstic acid (PTA) encapsulated MIL-101-Cr (50% PTA@MIL-101-Cr, here PTA was used as a representative HPA) using
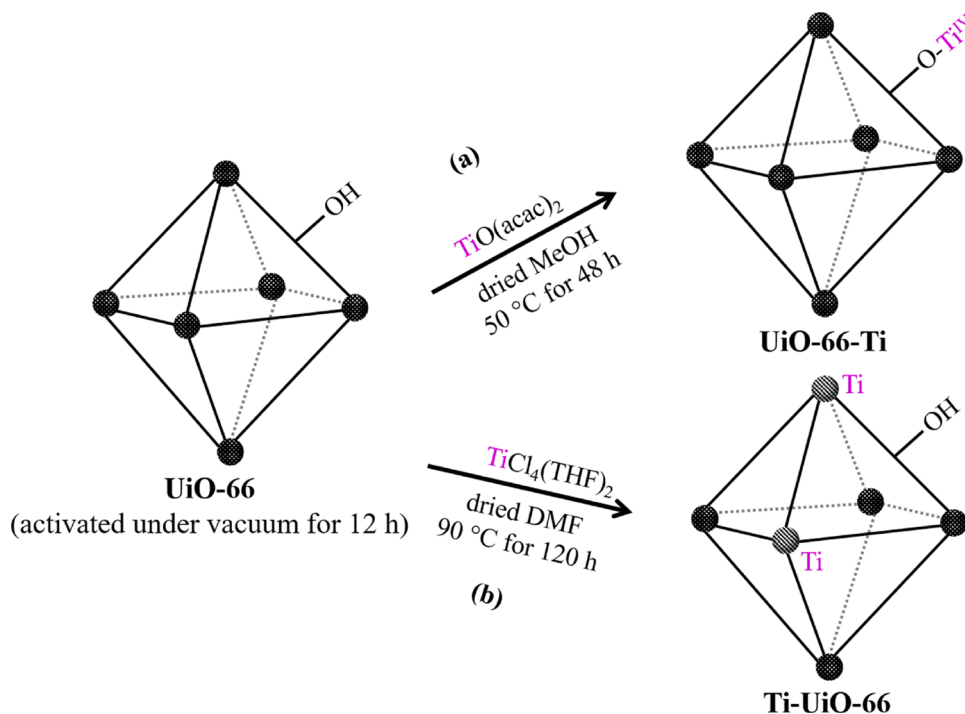

Fig. 7. Representation of the synthesis of Ti-UiO-66-Zr MOFs from UiO-66-Zr via Ti-exchange methods.
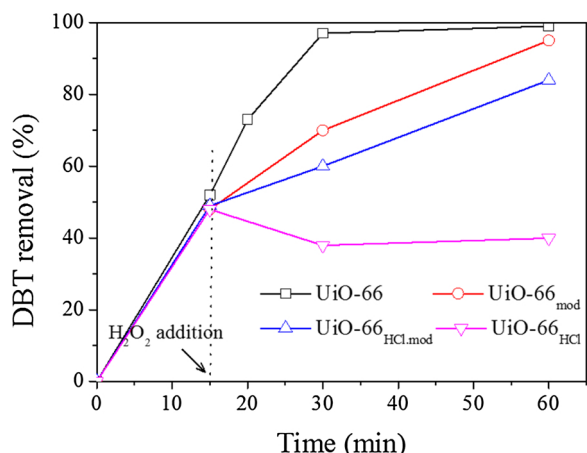
Fig. 8. Effect of time on the removal of DBT over the UiO-66, UiO-66$_{mod}$, UiO-66$_{HCl\cdot mod}$ and UiO-66$_{HCl}$ (Reproduced from Ref. [121], Copyright 2015 Royel Society of Chemistry).

one pot "bottle around ship" [26] approach (Fig. 10). The resulting materials showed remarkable efficiency in the removal (almost complete: ~ 99%) of DBT from a model fuel at 50 °C in the presence of H_2O_2 and DMF (as oxidant and extractant, respectively) along with a surfactant (CTAB, as a phase transfer agent) in 3 h. However, the ODS was done in the presence of a huge quantity of oxidant (H_2O_2/DBT = 50), which will decrease the general efficiency of the process. The material exhibited good recyclability and reusability up to four consecutive cycles which was also active in the oxidation of BT and 4,6-DMDBT. Meanwhile, MIL-101-Cr without POM was capable of removing DBT from the model fuel only by 9% under the studied conditions. Ribeiro et al. [142] demonstrated the oxidative removal of SCCs from N-O ctane

using tetrabutylammonium salt of PTA (TBA$_3$PW$_{12}$O$_{40}$)-encapsulated MIL-101 (named as, PW$_{12}$@MIL101-Cr). Here, the PW$_{12}$@MIL101 was prepared by post-impregnation (Fig. 11) of PW$_{12}$ into the MIL-101-Cr pores via stirring the MOF and PW$_{12}$, in a MeCN solvent, under ambient condition. The PW$_{12}$@MIL-101-Cr composite showed almost complete removal (~ 99%) efficacy for the studied BT derivatives within 1–4 h of reaction at 50 °C in the presence of oxidant H_2O_2 and an IL (1-butyl-3-methylimidazolium hexafluorophosphate) as extractant. The catalytic desulfurization over the PW$_{12}$@MIL-101-Cr was far superior to that of the simple extraction by the IL. Anion-exchange approach (Fig. 12) was also accomplished by using amino-functionalized MIL-101 (H$_2$N-MIL-101-Cr), after protonation of -NH$_2$ with HCl into -NH$_3^+$, as a support material to encapsulate PTA-anion into its cavity [143]. This method might be highly feasible to have stable composite materials via protecting the probable leaching out of small PTA-anion (~ 13–14 Å diameters) through the large window (16 Å) of the H$_2$N-MIL-101-Cr. Or, electrostatic interactions between PTA-anion and NH$_3^+$-cation of the H$_2$N-MIL-101-Cr could be created during the impregnation process; therefore, the composites might be stable during catalysis and reactivation, etc. As summarized in Table 3, the obtained PTA@H$_2$N-MIL-101-Cr showed excellent efficacy (complete removal in 1 h) for ODS of DBT from n-heptane with considerably high reaction rate (k_{app} = 7.6 × 10^{-2} min^{-1}) at 50 °C in the presence of H_2O_2 and MeCN. Moreover, the oxidation reactivity decreased in the order DBT (99.6%) > 4,6-DMDBT (88.2) > BT (70.5%), as shown in Fig. 12b. Fascinating recyclability with no loss of activity (or no leaching of active PTA species) was confirmed even after recycles for several times owing to the electrostatic interaction of PTA-anion and NH$_3^+$-cation of the H$_2$N-MIL-101-Cr. Using the same strategy, an efficient ODS catalyst (PTA@H$_2$N-MIL-53-Al) having relatively low activation energy (34.1 KJmol^{-1}) was also developed [144]. On the other hand, a recent report [145] showed a way to restrict the leaching of PTA from the PTA-encapsulated MIL-101-Cr (MOF without amine functionalization) via
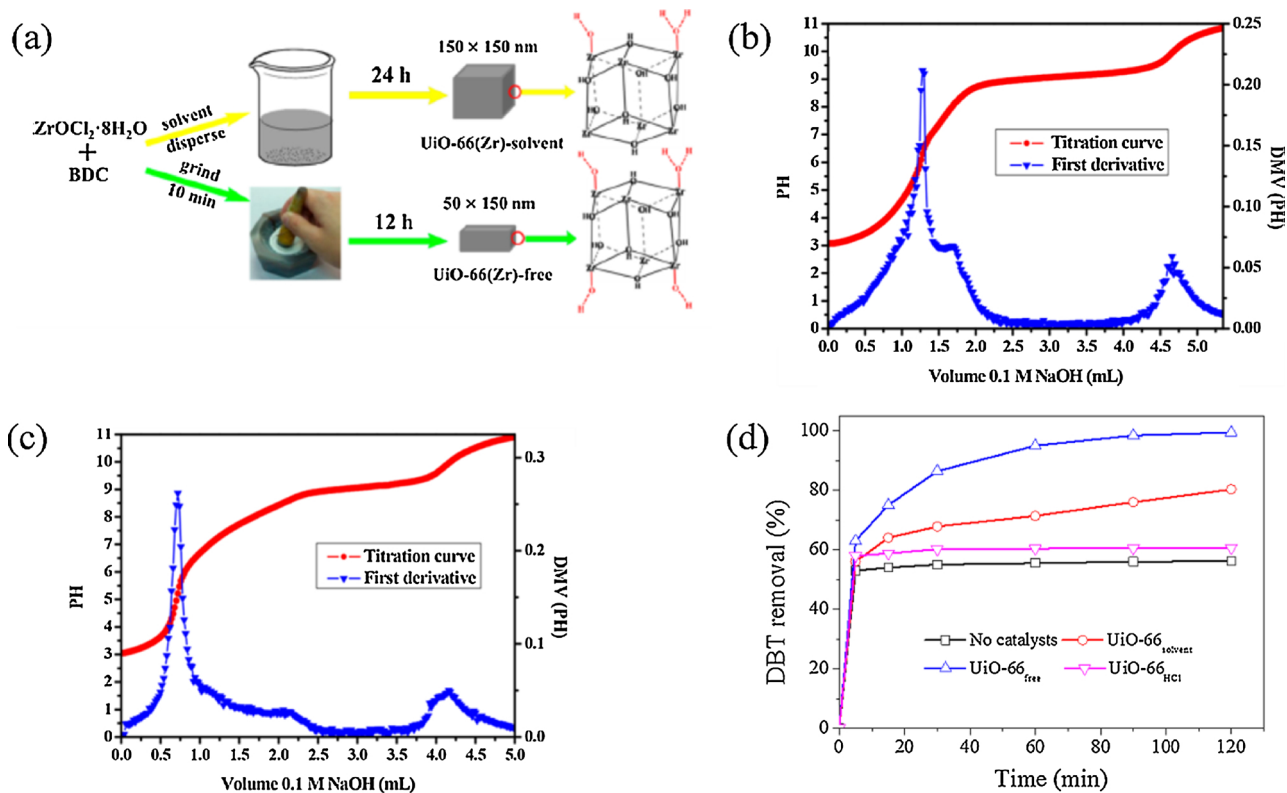

Fig. 9. (a) Schematic diagram about synthetic process of UiO−66-Zr under different conditions; Acid − base titration curve and first derivative curve for (b) UiO−66-Zr$_{solvent}$ and (c) UiO−66-Zr$_{free}$ and, (d) Removal efficiency of DBT with reaction time over various UiO-66-Zr catalysts (Adapted from Ref. [122], Copyright 2017 ACS).

Table 3

Summary of the studies on the oxidative desulfurization over active-species encapsulated-MOFs. The reaction parameters including the studied SCCs, oxidant, initial concentration of SCCs, catalyst dosage, oxygen-over-sulfur ration, reaction temperature, reaction time, conversion, kinetic constant and activation energy, and remarks (as footnotes) are shown in the Table.

Catalysts	SCC	Oxidant	Conc. of SCC (ppm)	Catalyst amount (g/L)	O/S ratio	Reaction temperature (°C)	Reaction time (min.)	Conversion (%)	Kinetic constant (min⁻¹)	Activation energy (KJ·mol⁻¹)	Ref.
50%PTA@MIL-101-Cr	BT DBT 4,6-DMDBT	H_2O_2	2684 3685 4246	7.5	50	50	180	~86 ~99 ~90			[141][a]
PW₁₂@MIL101-Cr	DBT	H_2O_2	18426	520	880	50	240	~99			[142][b]
PTA@H₂N-MIL-101-Cr	BT DBT 4,6-DMDBT	H_2O_2	950	5	~4	50	240	70.5 99.6 88.2	7.6×10^{-2}		[143][c]
PTA@H₂N-MIL-53-Al	DBT	H_2O_2	500	7	20	65	240	~100		34.1	[144][d]
PTA@MIL-101-Cr-diatomite	DBT	H_2O_2	500	8.3	5	60	120	~100			[145][e]
PMo@HKUST-1-Cu	DBT Th MPS	H_2O_2	500		6	65	150	~88 ~95 ~100			[147][f]
PTA@UiO-67-Zr	BT DBT 4,6-DMDBT	H_2O_2	1000	5	13	70	60	75 99.5 80			[148][g]
PMA@UiO-66-Zr	DBT	TBHP	500	4.5	3	80	60	~100			[149][h]
42%PTA@MOF-808A-Zr	BT DBT 4,6-DMDBT	H_2O_2	1000	3	5	60	60	82 ~100 42	1.6×10^{-1}	29.0	[150][i]
PTA@ZIF-8-Zn PTA@UiO-66-Zr PTA@MIL-100-Fe	DBT	H_2O_2	950	7.5	4	70	60	13 73 100			[151][j]
NENU-9-Cu	DBT	molecular oxygen	500	0.88		80	60	90			[152][k]

[a] Highly active ODS catalysts with high dispersion could be prepared by "bottle around ship" approach.

[b] Removal (~99%) of SCCs could be attained using IL as extractant.

[c] Very good recyclability without leaching could be achieved due to the electrostatic interaction of PTA with the ammonium groups of H_3N^+-MIL-101-Cr.

[d] Good recyclability with ~94% removal efficiency.

[e] Diatomite not only restrict the leaching of POM but also immobilize the active components for enhanced performance.

[f] Both the central (P or Si) and the coordinated atoms (Mo, or W) of the POM-based catalysts have important role in the ODS reactivity.

[g] Size-matched UiO-67-Zr successfully prevented the leaching of POM.

[h] Mo^{5+} of the PMA@UiO-66-Zr acted as the main active site for ODS reaction readily facilitated by the formation of •OH reactive species rather than the Mo^{6+}.

[i] Stable POM@MOF based catalysts can be prepared via tuning the window size.

[j] Window size–activity for ODS efficiency was observed and the leaching amount of PTA increased with the increasing of the window size.

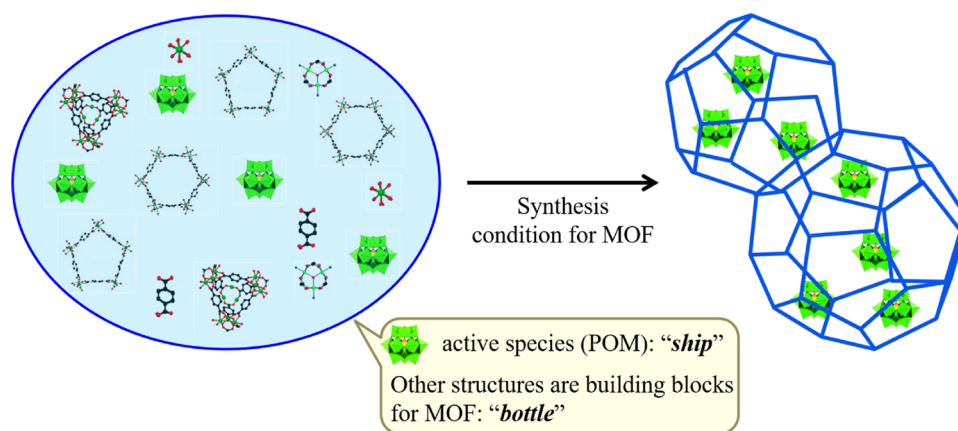[k] In-situ encapsulation of POM into a Cu-based MOF was also remarkable in ODS of DBT.

Fig. 10. Illustration of the in-situ synthesis of POM@MOF via "*bottle around ship*" method (Reproduced from Ref. [141], Copyright 2013 Elsevier).

MOF   **MOF-encapsulated with active species**
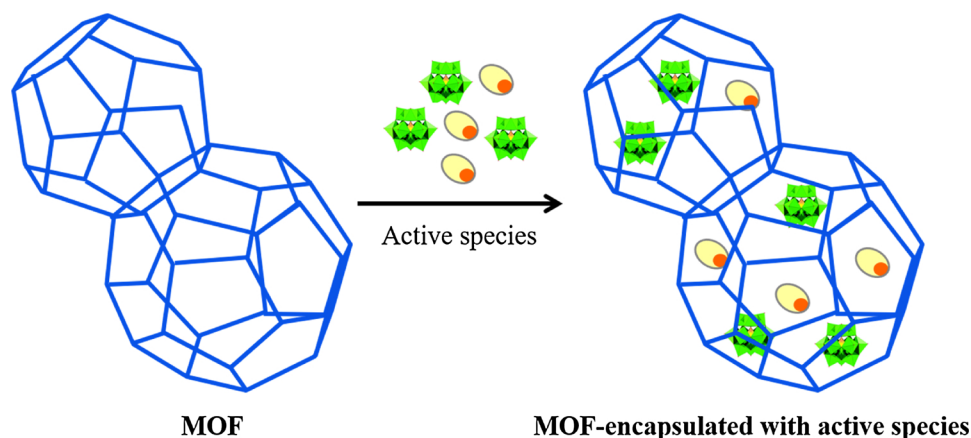
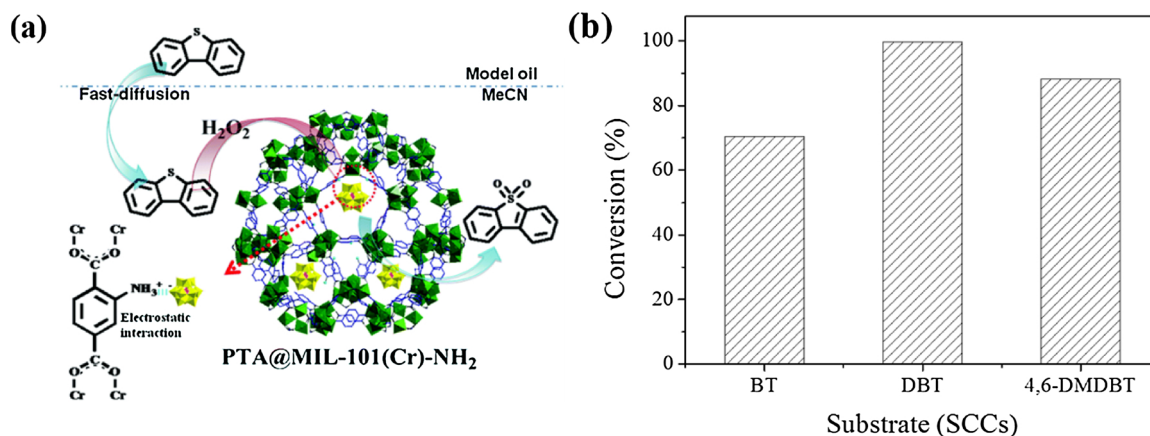**Fig. 11.** Scheme to show post impregnation of active species into MOF.

Fig. 12. (a) Anion exchange method for functionalization of MOF (here, PTA@H$_2$N-MIL-101-Cr) and (b) oxidative conversion of selected SCCs over the PTA@H$_2$N-MIL-101-Cr (Reproduced from Ref. [143], Copyright 2014 Royel Society of Chemistry).

preparing the composite in the pore of mesoporous diatomite using one-pot synthesis method. The PTA@MIL-101-Cr-diatomite material was observed as good catalysts especially in terms of ready recyclability with no loss of activity where diatomite plays a vital role in the immobilization of the active components. This strategy could stabilize the PTA or POM in the pores of MIL-101-Cr; however, SCCs could approach the active sites (PTA or POM) of the catalyst.

Along with MIL-101 s, some other MOFs having different metal centers (such as Cu, Co, Zr, Zn, Fe), for examples, [Co(BBPTZ)$_3$] [HPMo$_{12}$O$_{40}$]·24H$_2$O   (BBPTZ = 4,4'-bis(1,2,4-triazol-1-ylmethyl)

biphenyl) [146], HKUST-1 [147], UiO-67-Zr [148,149], MOF-808-Zr [150], ZIF-8-Zn, UiO-66-Zr and MIL-100-Fe [151], were also used as host to encapsulate active POM/HPA species into their pores to have improved ODS capabilities. NENU-9-Cu [(CH$_3$)$_4$N]$_2${[Cu$_2$(BTC)$_{4/3}$(H$_2$O)$_2$]$_6$-[H$_3$PV$_2$Mo$_{10}$O$_{40}$]}·14H$_2$O [152] is a special MOF with a well-defined crystal structure that is in-situ POM-encapsulated Cu-BTC. The size-controlled NENU-9 s were obtained by a suitable combination of reaction precursors; and, were applied in the oxidation of SCCs in the presence of molecular oxygen. The NENU-9-Cu with small size showed remarkable activity in a catalytic ODS reaction. A similar strategy was
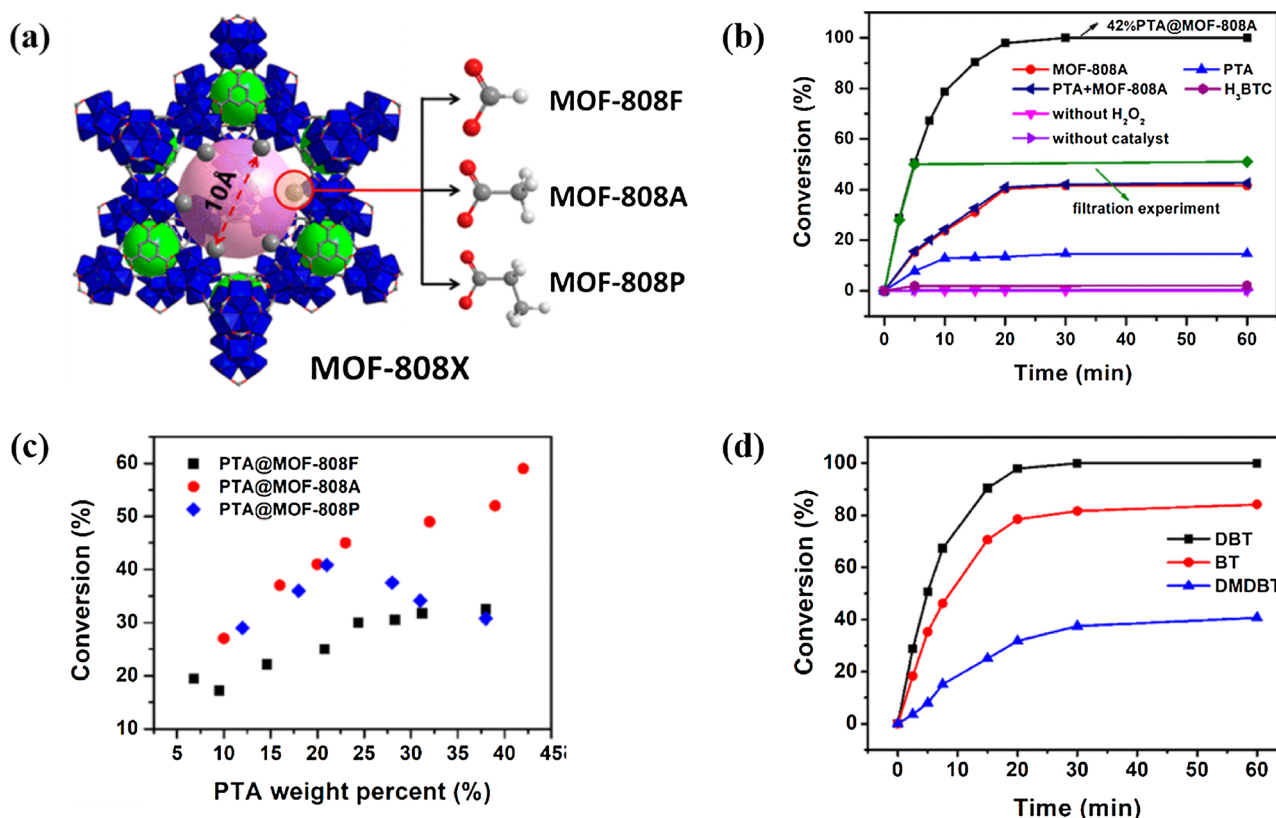
Fig. 13. (a) Structures of MOF-808-Zr(X) showing the hexagonal windows of 10 Å including the coordinated anions. (b) Effect of time on the removal of DBT using different catalysts, (c) PTA@MOF-808-Zr(X) composites with various PTA contents screened for the oxidative desulfurization of DBT at 60 oC for 10 min, and (d) effect of time on the conversion of BT, DBT and 4,6-DMDBT over PTA@MOF-808-Zr(A) (Adapted from Ref. [150], Copyright 2018 ACS).

applied to prepare a POM-encapsulated Co-based MOF ([Co(BBPTZ)$_3$] [HPMo$_{12}$O$_{40}$]·24H$_2$O) [146] that showed ˜100% conversion of DBT after 15 min of reaction in the presence of TBHP. Effect of the metal center of POMs or HPAs on the ODS was also studied by using three commercial HPAs including H$_3$PMo$_{12}$O$_{40}$ (PMo), H$_3$PW$_{12}$O$_{40}$ (PW or PTA) and H$_4$SiW$_{12}$O$_{40}$ (SiW) after incorporation in HKUST-1 (POM@ HKUST-1) by one-pot encapsulation method [147]. ODS reactivity of the three POM@HKUST-1 s was in the order: PMo@HKUST-1 > PW@ HKUST-1 > SiW@HKUST-1. This fact suggested that both the central atom (P or Si) and the coordinated atom (Mo, or W) of the POM-based catalysts have a vital role in the ODS reactivity. Or, P and Mo (as the central atom and the coordinated atom, respectively) had higher activity than the Si and W, respectively [153]. Consequently, POM consisting of Mo metal was suggested as a good catalyst for ODS reactions.

Very recently, a few POM@MOF-based ODS catalysts were developed to follow one-pot solvothermal or 'bottle around ship' approach using various MOFs including UiO-67-Zr, MOF-808-Zr, ZIF-8-Zn, UiO-66-Zr, and MIL-100-Fe. UiO-67-Zr possesses two types of cages with diameters of 11.5 Å and 18.0 Å (super-tetrahedral and super-octahedral, respectively) which could provide sufficient spaces to encapsulate the PTA (˜13 Å), while leaching of PTA was restricted by the small window (8.0 Å). Therefore, the PTA@UiO-67-Zr achieved a fascinating performance in ODS catalysis (for removal BT/DBT/4,6-DMDBT in n-heptane solvent, with H$_2$O$_2$ at 70 °C in 1 h) with good recyclability [148]. The removal efficiencies for BT, DBT, 4,6-DMDBT were different from one another owing to the differences in electron density [31,154] of S-atoms as well as the molecular size of the respective SCCs. The importance of electron density on the S atom of SCCs, which was observed in the mentioned study, will be discussed in the next part. Wang et al. [151] demonstrated the effect of window size of the MOFs on the efficiency of ODS over a series of PTA@MOF using three MOFs having different window sizes. For instance, ZIF-8-Zn, UiO-66-Zr, and MIL-100-

Fe have windows of 3.4 Å, 6.0 Å and 8.6 × 5.8 Å, respectively. Observed ODS activity over three PTA@MOFs (13%, 73% and 100% conversion of DBT over the PTA@ZIF-8-Zn, PTA@UiO-66-Zr and PTA@ MIL-100-Fe, respectively, in the presence of H$_2$O$_2$), prepared via encapsulation of PTA into their pores (by one-pot solvothermal method), revealed that the accessible window for the substrate is essential to get highly active ODS catalyst. This is understandable considering the effective interaction of SCCs with the encapsulated PTA (active site) is essential for ODS, very similar to the results observed with pristine MOFs.

Further study on the development of a PTA@MOF-based ODS catalyst (42%PTA@MOF-808A-Zr), having high activity and recyclability, was carried out (Fig. 13) via tuning the window size of a single MOF (MOF-808-Zr) through changing the length of coordinated monocarboxylate (e. g. formate (F), acetate (A) and propionate (P)) groups [150]. The large adamantane shape cage (18 Å) of the MOF-808X-Zr (X = F, A and P) could encapsulate PTA (˜13 Å) molecules which were restricted in the cages because of the smaller window sizes (11.8, 10.0 and 7.8 Å for MOF-808F-Zr, MOF-808A-Zr and MOF-808P-Zr, respectively), compared with the diameter PTA molecule. However, the windows are still as large as to accommodate the substrates to the encapsulated PTA or main active sites for efficient catalytic performance. The 42%PTA@MOF-808A-Zr was found to be the best catalysts among the prepared materials under the optimal reaction condition (60 °C in the presence of H$_2$O$_2$) in that study (Fig. 13b). The high activity of 42% PTA@MOF-808A-Zr (MOF with optimized PTA loading, Fig. 13c) was achieved by the contributions of an accessible window for the substrate (SCCs) to interact with highly dispersed active PTA along with the uniformly decorated Zr − OH in zirconium clusters. Again, the ODS efficiencies were dependent on the electron density of the S-atom of the studied SCCs, which will be discussed in the next part. On the other hand, very recently, Zhang et al. [149] reported phosphomolybdic acid

Table 4

Summary of the studies on the oxidative desulfurization over MOF-derived nanomaterials. The reaction parameters including the studied SCCs, oxidant, initial concentration of SCCs, catalyst dosage, oxygen-over-sulfur ration, reaction temperature, reaction time, conversion, kinetic constant and activation energy along, and remarks (as footnotes) are shown in the Table.

Catalysts	Precursor MOF	SCC	Oxidant	Reaction temperature (°C)	Reaction time (min.)	Conversion (%)	Kinetic constant (min^{-1})	Activation energy $(KJ \cdot mol^{-1})$	Ref.
TiO$_2$/NC	IRMOF-3-Ti(O-iPr)4)	DBT	TBHP	100	60	–	3.4×10^{-3}		[165][a]
C-600	MIL-47-V	DBT	TBHP	104					[166][b]
C-1000									
C-1100									
MDC-C	ZIF-8@H2N-MIL-125-Ti	Th	H$_2$O$_2$	80	120	48	1.4×10^{-2}	–	[167][c]
		BT				59	2.0×10^{-2}	–	
		DBT				~100	1.2×10^{-1}	19	
		2,6-DMDBT				38	7.3×10^{-3}	–	
TiO$_2$/C	Meso-MIL-125-Ti	DBT	TBHP	80					[168][d]
TiO$_2$@M6	TiCl4@MAF-6-Zn	DBT	H$_2$O$_2$	80	60	97.4	5.0×10^{-2}	23.3	[39][e]
TiO$_2$@M-74	Ti(SO$_4$)$_2$@MOF-74-Zn	DBT	H$_2$O$_2$	80	60	84.4	3.2×10^{-2}	27.0	
MnO@porous carbon	MOF-74-ZnMn	DBT	H$_2$O$_2$	80	120	96	5.8×10^{-2}	–	[98][f]

[a] Well-dispersed tiny TiO$_2$ particle and high surface area influenced the high ODS activity.
[b] V-carbide rather than V-oxide can provide enhanced chemical stability during ODS reaction.
[c] Uniformly dispersed smaller TiO$_2$ nanoparticle and wide mesoporosity of the materials revealed the higher activity.
[d] Ti oxycarbide was the main active sites for improved oxidation with a strong function of the mesoporosity.
[e] Well-dispersed rutile TiO$_2$ along with synergistic effect of doped N-atom influenced the ODS performance.
[f] Well-dispersed MnO and high porosity with mesopores were responsible for the high activity.

(PMA)-encapsulated UiO-66-Zr (PMA@UiO-66-Zr), which showed a very high efficiency for ODS of DBT from decalin in the presence of TBHP. The 10% PMA@UiO-66-Zr composite (that calcined at 200 °C) demonstrated a promising efficacy (~100% DBT or 4,6-DMDBT conversion in ~60 min), where Mo^{5+} (rather than Mo^{6+} that was reduced to Mo^{5+}) of the PMA was assumed as the main active site for the ODS reaction.

Incorporation of IL into MOFs (via simple impregnation) also increased the performances in ODS reaction [144]. The ODS was conducted for BT dissolved n-heptane solution in the presence of H$_2$O$_2$ at the temperature ranges from 30 to 50 °C with a successfully prepared IL (1-methylimidazolium-3-propylsulfonate hydrosulfate)-impregnated UiO-66-Zr. The 40%IL@UIO-66-Zr showed BT removal efficiency of 94.6%, which was improved from the efficiency (~84%) of pristine UiO-66-Zr; and could be recycled readily without loss of performance.

Therefore, active species (such as POM/HPA and IL)-loaded MOFs can be suggested as good catalysts for ODS to remove various SCCs from fuels, quite similar to the ADS with an adsorbent with the tri-component of POM, IL and MOF [136]. There are several strategies including one-pot (or bottle around ship) syntheses and post-loading (via impregnation, etc.) to prepare various POM or IL@MOFs-based catalysts for ODS. The properties, as well as the activity, can be tuned by selecting MOFs (with suitable cavity or cage and window sizes), ILs (with adequate active sites), and POMs (with suitable active sites). Moreover, POM or IL@MOFs were found to be recyclable up to several cycles. However, there might have a chance to leaching out of the POM or IL from the composite materials especially when the host MOFs have a window with size larger than the size of loaded active species. In that case, the possible leaching might be prevented or controlled via a special chemical interaction such as electrostatic ones (for example, as discussed above, between anion of POM and cation of MOF).

2.4. Oxidative desulfurization over MOF-derived carbonaceous materials

Recently, MOFs have been found as an ideal precursor to prepare various hetero atom-doped functional materials that are highly effective in various applications including heterogeneous catalysis [99–102,155] and adsorption [102,156–164]. There are a few studies on the ODS using carbonaceous materials obtained via carbonization of

pristine, post-modified, composite and bimetallic MOFs. Here, we summarize (Table 4) their ODS efficiency along with the preparation of such advanced materials.

Considering the activity of Ti- and V-based materials in the ODS reactions, the MOFs composed of Ti or V were mainly used as a precursor to develop MOF-derived ODS catalysts [39,98,165–167], even though Mn-based MOF-derived carbon was also found as an effective catalyst for ODS [98]. So far, Kim et al. firstly studied the ODS of DBT using a TiO$_2$-nanoparticle supported on nanoporous carbon (TiO$_2$/NC) that derived from carbonization of IRMOF-3-Zn/Ti or IRMOF-3-Zn {Zn$_4$O(H$_2$N-BDC)$_3$}$_2$ modified with titanium isopropoxide via post-synthesis (Fig. 14) [165]. The high-temperature carbonization (1000 °C for 6 h) of the IRMOF-3-Zn/Ti resulted in the TiO$_2$/NC nanohybrid material (after selective removal of Zn-metal) having very well distributed tiny TiO$_2$ nanoparticles (size: 4 nm) with high surface area (1060 m^2/g) and large mesopore volume (1.19 cm^3/g). The obtained TiO$_2$/NC nanohybrid material showed good efficiency in the oxidation of DBT from a model fuel with TBHP oxidant. The TiO$_2$/NC catalyst exhibited a much higher catalytic activity with $k_{app} = 3.4 \times 10^{-3} min^{-1}$ than that of the TiO$_2$/AC ($8.0 \times 10^{-4} min^{-1}$) and showed very good stability or maintained its catalytic activity even after several cycles.

TiO$_2$/C based materials, which was prepared via carbonization of a Ti-based MOF (MIL-125-Ti), was also applied for ODS of fuel [168]. Products of pyrolysis of Zn-based MOFs have relatively high surface areas or pore volumes; however, the porosity of products from pyrolysis of other metals-based MOFs is generally low [102]. This is easily understood because of the high boiling points of produced metals (excluding Zn) or metal oxides. To overcome these limitations, a hierarchical microporous/mesoporous analogue of microporous MIL-125-Ti was synthesized and subjected to pyrolysis at various temperatures. By varying the pyrolysis temperature, both Ti content and phase in the final materials could be controlled (Fig. 15a). The resulting materials exhibited enhanced mesoporosity and activity in the DBT oxidation, compared with the catalyst obtained via pyrolysis of conventional microporous MIL-125-Ti (Fig. 15b). This increased activity was attributed to the higher mesoporosity of the hierarchical materials.

In addition, Bhadra et al. [167] developed a TiO$_2$-decorated carbon (named MDC-C) (with uniformly dispersed TiO$_2$ nanoparticles) via
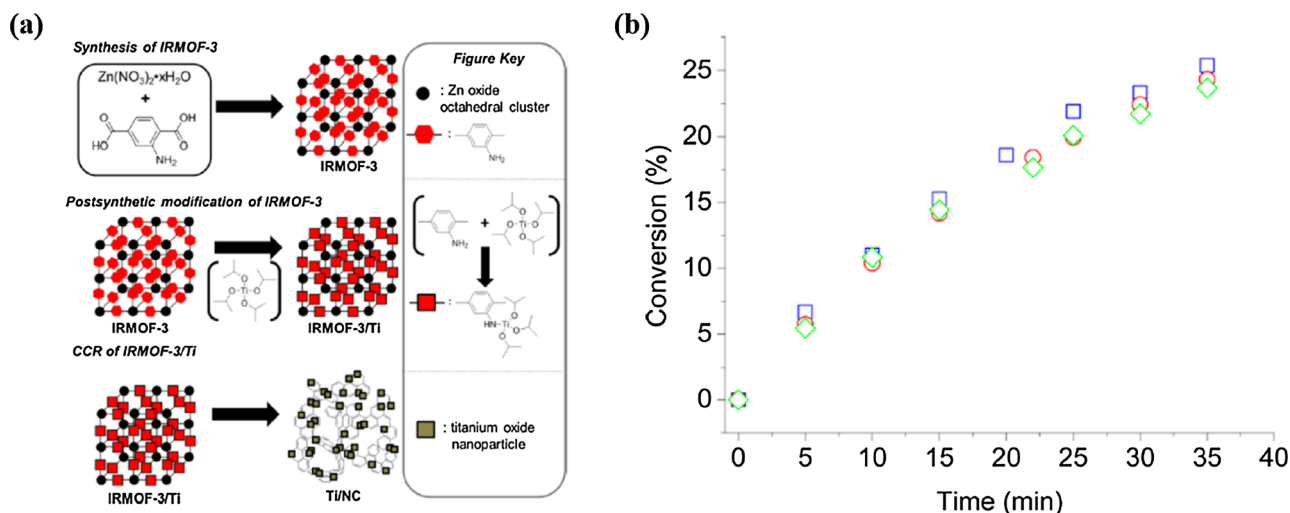
Fig. 14. (a) Modification and carbonization of IRMOF-3 and (b) ODS performance over the obtained TiO$_2$-decorated carbon (Adapted from Ref. [165], Copyright 2013 ACS).

carbonization of a composite MOF (ZIF-8-Zn@H$_2$**N**-MIL-125-Ti) at 1000 °C. Uniformly dispersed TiO$_2$ nanoparticles (~8 nm) onto mesoporous carbon support having high surface area could be achieved by the selective removal of the by-produced Zn-metal (a constituent of ZIF-8-Zn) during the carbonization process (Fig. 16). The material (MDC-C) showed outstanding catalytic performance for ODS with H$_2$O$_2$ oxidant, in terms of a low catalyst dose and fast kinetics, even at lower concentrations of the active species (TiO$_2$), compared with other TiO$_2$-based catalysts (both prepared and commercial catalysts) (Fig. 17a). The efficient catalysis for ODS could be explained by the large mesopores of MDC-C and the well-dispersed/small-sized TiO$_2$.

Very recently, Sarker et al. [39] prepared TiO$_2$ nanoparticle-integrated porous carbon via carbonization of MOFs loaded with TiCl$_4$ (as Ti precursor) by applying double solvent method (Fig. 18a). It was demonstrated that the properties of TiO$_2$-decorated carbons could be tuned by carbonization after controlled loading of Ti-precursor (inside or outside of MOFs) into suitably selected MOFs and solvents (to dissolve Ti precursors), based mainly on the hydrophilicity or hydrophobicity. The material that obtained from the TiCl$_4$@MAF-6-Zn (TiO$_2$@M6) (where MAF-6-Zn was a hydrophobic MOF that dispersed in hydrophilic DMF to which hydrophobic N-O ctane dissolved with TiCl$_4$ was added) showed remarkable activity in ODS of DBT (Fig. 18b), in terms of high rate constant (5.0×10^{-2} min^{-1}) and low E$_a$ (23.3 kJ·mol^{-1}), in the presence of H$_2$O$_2$ (as oxidant) and MeCN (extractant) at 80 °C. Again, the role of uniform dispersion of smaller TiO$_2$ nanoparticles onto highly porous carbon was suggested as an influential factor for the high efficacy in the ODS.

Furthermore, a series of V-based carbon catalysts for ODS was prepared through carbonization of MIL-47-V [166]. By this method, substantial leaching of active V species, especially in liquid-phase oxidation reactions, might be restricted by in-situ production of active V-species onto the mesoporous carbon support. The phases of V-species could be controlled by optimizing the carbonization temperature. The materials showed comparable performances in ODS, and the efficiencies along with leaching of V-species during the ODS process (in several cycles) were dependent on the phases of V-species that produced upon carbonization. For instance, the activity of ODS follow the order: C1000(V^{3+} and V^{8+}) > C600(V^{3+}, V^{4+} and V^{5+}) > C1100(V^{8+}). Curiously, the performances of C1000 and C1100 increased in the second or third cycles even after significant loss of V-species in each recycling processes. Considering the lowest loss of V-species from C1100 in the ODS reaction, C1100 was suggested as a stable V-based ODS catalyst even with lower activity. On the other hand, based on the observed results, V^{4+} and V^{5+} oxide species were suggested as the main active component for ODS. However,

interestingly, C1100 having inactive V^{8+}(V-carbide) species was found to be also active in ODS. These results suggested the occurrence of the simultaneous transformation of V-carbide (V^{8+}) into active V^{4+}/V^{5+} (that can oxidize DBT effectively) and leaching of V-species after subsequent oxidation of the DBT. In addition, MnO-doped mesoporous carbon, derived from a bimetallic MOF (MOF-74-Zn/Mn), also was found to be active in ODS of DBT (Fig. 19) from N-O ctane in the presence of H$_2$O$_2$ and MeCN (as oxidant and extractant, respectively) where Mn(II) might be the active component. Moreover, the ODS efficiency could be high, via the optimizing the Mn/Zn ratios of the MOF precursors (for pyrolysis), because of the tiny MnO nanoparticles and wide mesopore of carbonaceous materials [98].

Therefore, it can be assumed that MOF-derived carbon nanohybrid materials, that obtained via carbonization of MOFs (with or without modification), are very attractive for ODS of fuel, similar to MOFs (pristine or defected) and active component (POM/HPA or IL)-loaded MOFs. The size, distribution, and phase of nanoparticle (active component) play the main role in the ODS reaction; however, surface area and mesoporosity also have an influential role in the improved activity. The properties or activity of the MOF-derived nanomaterials could be tuned via controlling the carbonization conditions (especially temperature and atmosphere) and selecting/designing suitable MOF precursors.

3. Oxidative denitrogenation

The progress of the studies on ODN is much slower as compared with that on ODS, possibly because of the complex oxidation process of NCCs, that originated from the chemical properties of NCCs, compared to SCCs. The N atom on NCCs and S atom on SCCs are second-row and third-row elements, respectively; therefore, smaller N can accommodate only one oxygen atom, if any; however, larger S can have maximum two oxygen atoms, during the oxidation process. Or, nitrogen can rarely be oxidized into N oxides in fuel, whereas S can be easily oxidized into sulfone or sulfoxide. Moreover, during ODN, catalysts might be deactivated especially by the very reactive NCCs (especially, basic NCCs) that can react very strongly with common metal-based catalysts (even though SCCs also might poison some catalysts); thereby, difficult to find suitable catalysts or method for ODN. Therefore, only a few studies focused on ODN, so far. This chapter comprised of the reported results on ODN (Table 5) using various types of catalysts, including MOF-based ones, or methods.

In the early of the 21st century, Shiraishi et al. [41] firstly studied the denitrogenation of aniline, indole, and carbazole by a chemical process via alkylation and a subsequent precipitation method using
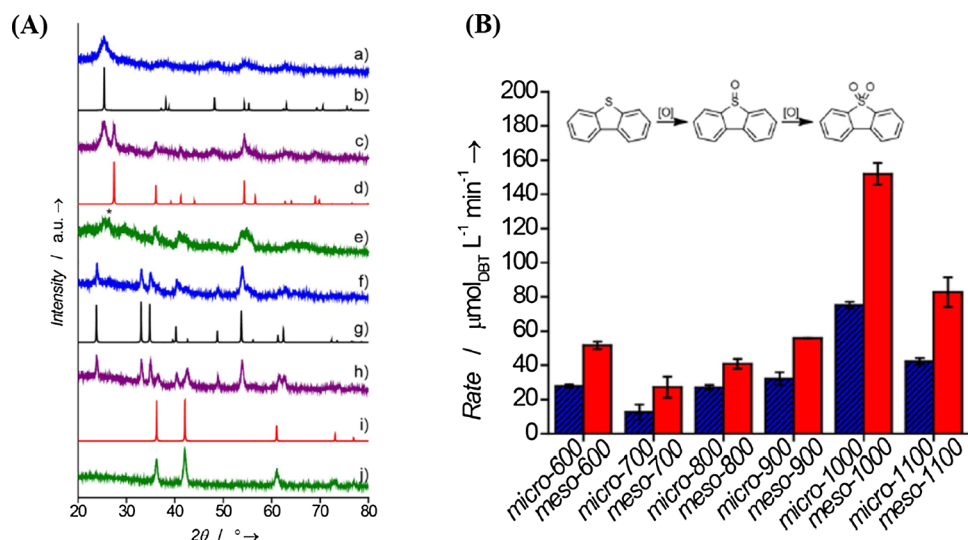
(A)

(B)

Fig. 15. (A) XRD patterns of MIL-125-Ti materials pyrolyzed at (a) 600, (c) 700, (e) 800, (f) 900, (h) 1000, and (j) 1100 °C along with the ICDD powder diffraction patterns of (b) anatase, (d) rutile, (g) Ti$_2$O$_3$, and (i) Ti carbide phases. The asterisk (∗) denotes a peak attributed to the suboxide Ti$_3$O$_5$ and (B) reaction rates of the oxidation of DBT catalyzed by the micro-temp (blue) and the meso-temp (red) series of materials in the presence of TBHP (where, 'temp' means the pyrolysis temperature of the MOFs) (Adapted from Ref. [168], Copyright 2016 ACS).
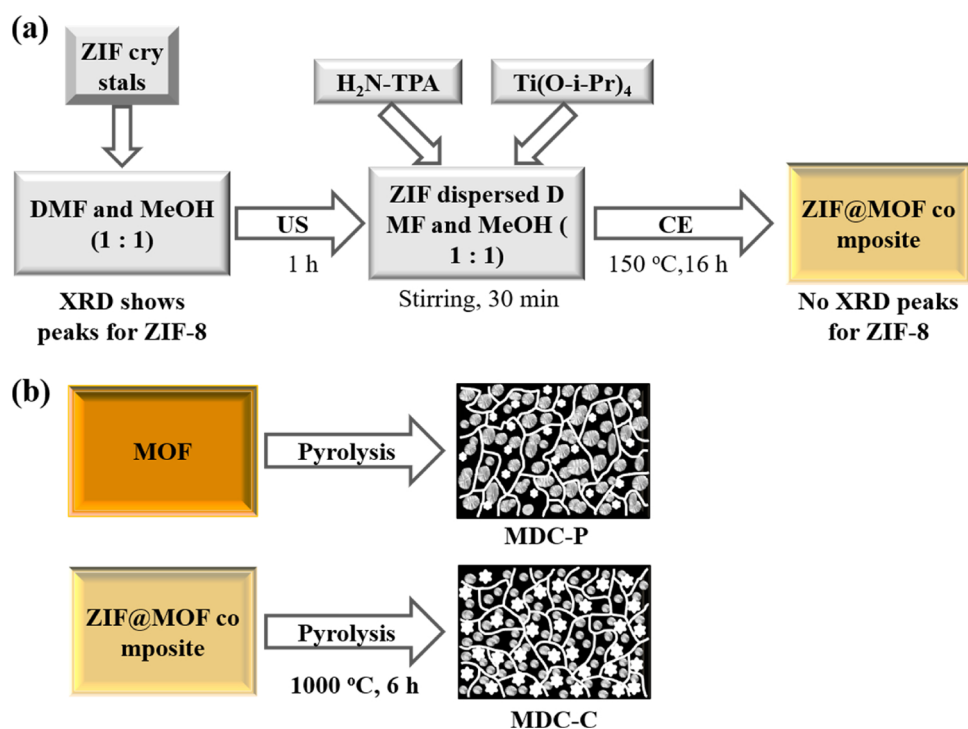
(a)

(b)

Fig. 16. Schematic diagrams for the (a) synthesis of ZIF@MOF composites, where, ZIF: zeolitic imidazolate fremawork-8 and MOF: H$_2$N-MIL-125 and (b) pyrolysis of MOF and ZIF@MOF where dark yellow: MOF; bright yellow: ZIF@MOF; black: carbon; gray: TiO$_2$; white stars: mesopores; white lines: micropores (Adapted from Ref. [167], Copyright 2018 ACS).
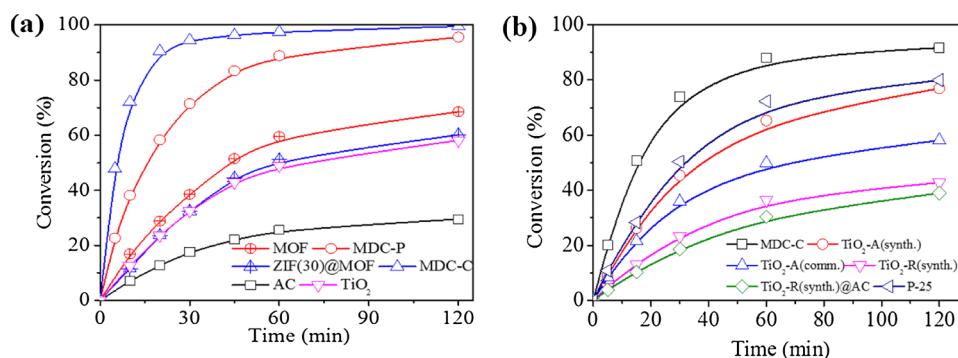
(a)

(b)

Fig. 17. Oxidative (a) desulfurization of DBT and (b) denitrogenation of IND over MDC-C along with a series of conventional TiO$_2$-based catalysts (Reproduced/adapted from Ref. [50,167], Copyright 2019 Elsevier and 2017 ACS).
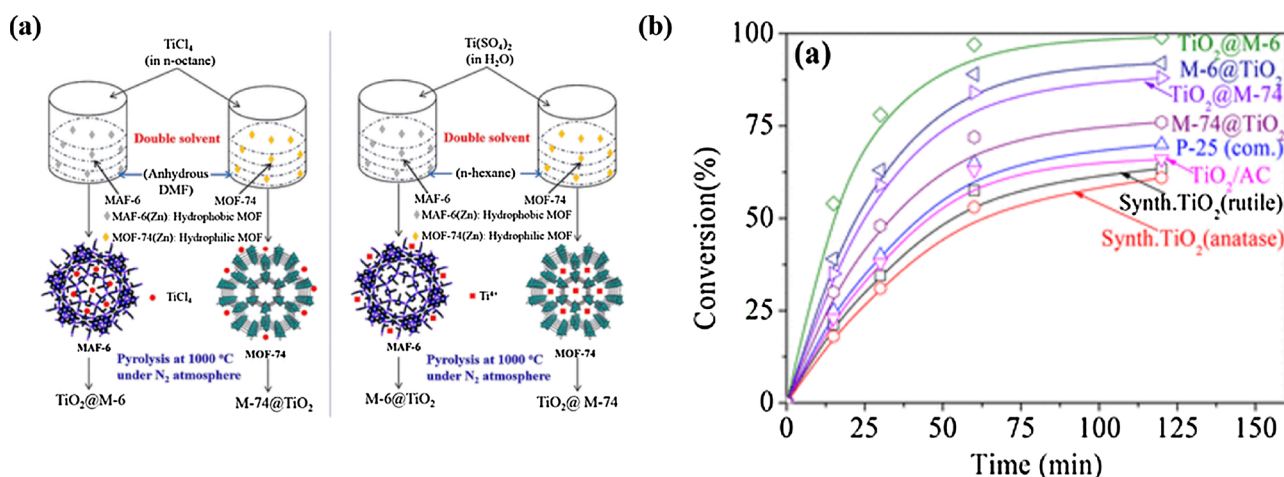
Fig. 18. (a) An illustration for the synthesis of TiO$_2$-decorated carbon and (b) effect of time on conversion of DBT (considering both adsorption and catalysis) over synthesized TiO$_2$ (rutile and anatase), commercial P-25, TiO$_2$/AC, and TiO$_2$-decorated carbons at 80 °C (Adapted from Ref. [39], Copyright 2019 ACS).
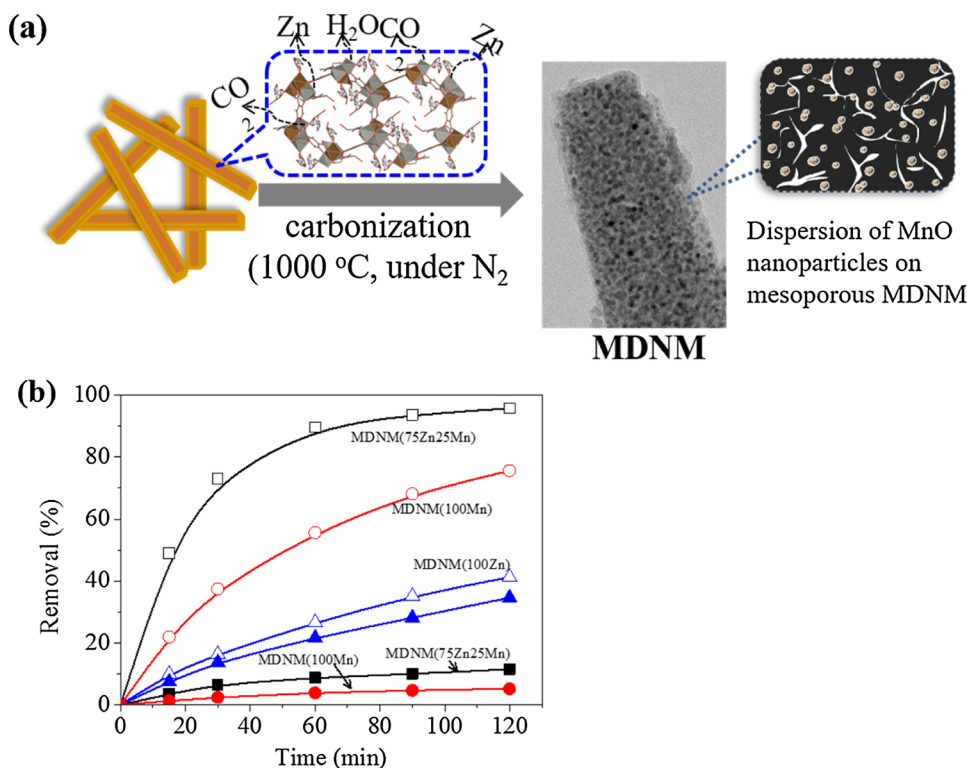

Fig. 19. (a) Representation for the synthesis of MnO-decorated carbon and (b) effect of time on the oxidative removal of DBT (considering both adsorption and catalysis) over a series of MnO-decorated carbon (Reproduced from Ref. [98], Copyright 2018 Royel Society of Chemistry).

AgBF$_4$ and CH$_3$I (as alkylating agents) from a xylene solution (as a model fuel). Later on, chemical oxidation followed by liquid-liquid extraction was found by the same group to be an alternative means to the alkylation/precipitation method. They could find ODN (from ani-line, indole, and carbazole solution in *n*-tetradecane or xylene solvent) was an effective method by using H$_2$O$_2$ or CH$_3$COOH (as oxidants) and MeCN/water azeotrope (as extractant), where no heterogeneous cata-lyst was used. After the reactions, oxidized aniline and CBZ were ex-tracted in the polar phase as azoxybenzene and carbazole-1,4-dione. However, the oxidized product of IND was a polymerized material ra-ther than the expected indoxyl or isatin [169], where chain poly-merization of indole might be occurred because of the high electron density of unsaturated C$_2$-C$_3$ bond. In a similar way, Nunes et al. [170] investigated the simultaneous removal of SCCs and NCC (here QUI was

the model NCC) under ultrasound irradiation (with CH$_3$COOH or H$_2$O$_2$ as oxidant; and with MeOH as extractant). The observed higher removal efficiency of QUI (up to 97%), compared to SCCs, from QUI-SCC mixed substrates suggested that QUI possibly was oxidized more preferably than the SCCs in the studied condition. Moreover, the role of extraction by the CH$_3$COOH and MeOH was suspected as a possible cause of higher nitrogen-removal efficiency, although the oxidized product of QUI was identified as QUI- N-O xide. Carnaroglio [42] investigated the ultra-sound irradiation for the ODS along with ODN using a series of oxidants including H$_2$O$_2$, Oxone (potassium peroxymonosulfate or a triple salt composed of KHSO$_5$, KHSO$_4$, and K$_2$SO$_4$), KO$_2$ and Na$_2$S$_2$O$_8$ in the presence of CH$_3$COOH. Among the used oxidant, Oxone was demon-strated as the best one to remove NCCs from fuel, and it can oxidize NCCs even in the absence of CH$_3$COOH. The influential role of

Table 5
Summary of the studies on the oxidative denitrogention over a variety of catalysts. The reaction parameters including the studied NCCs, oxidant, oxygen-over-nitrogen ration, reaction temperature, reaction time, conversion, and remarks (as footnotes) are shown in the Table.

Catalysts	Surface area (m^2/g)	NCCs	Oxidant	O/N ratio	Reaction temperature (°C)	Reaction time (min.)	Conversion (%)	Ref.
MoO_3/Al_2O_3		IND	TBHP	15			80	[44][a]
		QUI					68	
		Acridine					66	
		CBZ					45	
MoO_3/Al_2O_3		CBZ	TBHP	5	90	420	74.3	[45][b]
		QUI	$CH_3COOH + H_2O_2$		US-irradiation	9	97	[170][c]
		Basic-NCCs	$HCOOH + H_2O_2$	3	40 (US-irradiation)	2	95.85	[43][d]
PMo		Basic-NCCs	H_2O_2		40	30	75.2	[46][e]
VO(sal-HBPD)		QUI	H_2O_2	7	50		~100	[47][f]
V_2O_5/SiO_2	67.4	QUI	TBHP	7	70	720	80	[48][g]
g-C_3N_4/MIL-100-Fe	33	PRD	O_2	–	Xenon-lamp	360	~68	[49][h]
MDC-C	374	PRL	H_2O_2	10	50	120	44	[50][i]
		IND					92	
		1Me-IND					73	
		2Me-IND					89	
		3Me-IND					76	
		CBZ					14	

[a] Continuous flow process was applied to study ODN where CBZ was most difficult to oxidize.
[b] High selectivity was observed.
[c] NCCs were oxidized more effectively than the SCCs.
[d] Alcohol was used as extractant to extract oxidation products.
[e] The denitrification rate reaches up to 75.2% under the optimum denitrification condition.
[f] Very high selectivity was observed.
[g] The generation of OH• radicals was responsible for the oxidation of quinoline.
[h] Photoexcited electron-hole pairs originated the oxidation of PRD in n-octane.
[i] MDC-C might be a very promising catalyst in ODN and the oxidation efficiency increased with increasing electron density on the nitrogen of the INDs.

ultrasound irradiation was further observed by using HCOOH and H_2O_2 as oxidation media for the removal of basic NCCs [43].

Ishihara et al. [44] further studied the ODN reactivity of NCCs including carbazole, acridine, indole, and quinoline in decalin over a Mo-based heterogeneous catalyst (MoO_3/Al_2O_3) in the presence of TBHP oxidant at 80 °C using a fixed-bed flow reactor. The reactivity of tested NCCs for ODN was found in the order: indole > quinoline > acridine > carbazole, showing that the carbazole is most difficult to oxidize. On the other hand, Mo(VI)-complex (molybdenum acetylacetonate) showed slightly better performance (22.1% conversion) than the MoO_3 (10.8%) in the oxidative removal of CBZ from decalin in the presence of TBHP at 90 °C [45]. Considering the solubility of the complex in hydrocarbon, CBZ oxidation efficiency was also checked using prepared Mo(VI)-complex, after supporting on Al_2O_3 or resin; however, the performance was reduced rather than the expected increase. In contrast, MoO_3-supported on Al_2O_3 or resin boosted up the catalytic performance up to 74.3%, although the Mo-content was higher than that of the Mo(VI)-complex on Al_2O_3 or resin support. In addition, the phosphomolybdic acid was found to be an effective catalyst for the ODN of basic NCCs from fuel in the presence of H_2O_2 where alcohol could be used as extractant [46]. However, unfortunately, no firm conclusion on ODN could be reached based on the mentioned researches.

Recently, Ogunlaja et al. [47] studied ODN of QUI using a V-based catalyst (vanadium-coordinated N,N-bis(o-hydroxybenzaldehyde)phenylene diamine, or, [VO(sal-HBPD)]) in the presence of H_2O_2 (as an oxidant) and imidazoline-based ionic liquid (as extractant) at 70 °C. The developed catalysts effectively oxidized the QUI into QUI- N-O xide with a 100% selectivity by forming hydroxyl-peroxidovanadium(V) active species via reacting with the oxidant (H_2O_2). Moreover, another V-based catalyst (silica-supported V_2O_5) was used for studying the ODN of QUI from fuel in the presence of TBHP (as an oxidant) and ethanol (as extractant) at 70 °C [48]. The results demonstrated a high conversion of QUI (~80%) via reacting with the active OH• radical that was possibly formed by the activation of TBHP with the V_2O_5. The detailed mechanism for the oxidation of QUI will be described in the mechanism section.

In recent days, MOF-based or -derived catalysts were also being used in studying ODN [49,50]. Huang et al. [49] recently reported the photocatalytic ODN of pyridine in N-O ctane over protonated graphitic carbon nitride (PCN)-coated MOF (PCN/MIL-100(Fe)) using molecular oxygen as oxidant. The 44%PCN/MIL-100-Fe showed much better efficiency than the pristine graphitic carbon nitride and PCN, although the PCN was the main active species for the photocatalytic oxidation reaction in that study. Moreover, because of the high dispersion of coated PCN over the MIL-100-Fe, efficient separation of photoexcited electron-hole pairs is expected; therefore, improved photocatalytic activity in the oxidation of pyridine in N-O ctane could be accomplished. Additionally, Bhadra et al. [50] systematically studied ODN of a series of NCCs (INDs, PRL, QUI and CBZ) in N-O ctane over a composite-catalyst (MOF composite-derived TiO_2-decorated carbon or MDC-C that was found as a highly active catalyst for ODS, as illustrated in Fig. 17a [167]) in the presence of H_2O_2 (as oxidant) and CH_3COOH (as extractant) at 50 °C. The MDC-C was found to be a superior catalyst in its activity (or turnover frequency) for ODN among the prepared and commercial TiO_2-based catalysts (Fig. 17b). Moreover, INDs (normal and methyl-substituted) were more preferably oxidized than PRL and CBZ; however, QUI was not oxidized under the studied condition. A plausible mechanism was also suggested based on the oxidation rate and electron density of the N-atoms on the studied NCCs. The detail suggested mechanisms will be elaborated in the mechanism chapter.

Therefore, it can be concluded that ODN might be one of the promising methods to remove NCCs from fuels, similar to ODS. However, so far, only a few catalysts were developed and applied for ODN. Considering the possibility of ODN (however, progresses on the ODN is very little) and rapid development on MOFs or MOF-derived materials, ODN, especially with MOF-based or -derived catalysts, will be an attractive/promising research topic in the near future.

4. Mechanisms for oxidative purification of fuel

At present, there are a number of highly porous catalysts based on MOFs or derived from MOFs and oxidative purification (especially ODS) with those catalysts; however, still, there is a lack of sufficient

understanding on the reaction mechanism for ODS and ODN. Several factors including the type of used oxidants, active species as well as the properties of substrates (especially electron density on the S-atoms of the studied SCCs) can be considered to discuss the ODS mechanisms. In this review, we summarized the developed progresses on the reaction mechanism mainly for ODS by MOFs (pristine or post-functionalized) or MOF-derived catalysts having different active centers.

Oxidation reactions mediated with peroxides (e.g. CHP, TBHP and H_2O_2) are generally interpreted with two different reaction mechanisms [171]. The first mechanism is based on the one-electron process or the formation of free radicals that involves homolysis of peroxides (Scheme 1a) [118,171]. Another one is based on the two-electron process or a heterolytic reaction pathway (Scheme 1b) that can be obtained via increased electrophilicity of peroxides by the contribution of the catalyst [171,172]. Catalysts with active metal center including Mn, Fe, Co and Cu (group VIIA, VII1A, and 1B metals, respectively) generally go through the free radical mechanism via homolytic cleavage of peroxides. On the other hand, another group of catalysts having transition metals, such as Ti, V, Mo and W (group IVA, VA, and VIA metals, respectively), can promote the heterolysis of the $O-O$ bond in the peroxide intermediates such as metal-peroxo species. Metals having low oxidation potentials can be superior oxidation catalysts. For instance, the general activity order is Mo(VI) > W(VI) > V(V) > Ti(IV) [171]. However, properties of support materials (constituents, heteroatom dopants, porosity, and etc.) and active species (coordination number, particle size, and distribution) may also influence the efficacy of the transition metal-based catalysts. In addition, liquid-phase oxidation by using molecular oxygen with transition metal-based catalysts has been frequently explained via the free radical chain processes which is also called as "auto-oxidation" [115,171].

Similar mechanisms (Scheme 1) could be suggested for the catalytic ODS reactions over the various types of transition metal-based catalysts, although different mechanisms could be proposed/achieved depending on the physicochemical properties of the materials. During the ODS reactions, electrophilic addition of active oxygen atom (that generated from the interaction of peroxides with active metal-sites of the catalysts) to the S-atom of the heterocyclic SCCs generally occurred, which resulted in respective sulfoxides or sulfone as the oxidized products. Consequently, electron density on the S-atom of the heterocyclic SCCs greatly influences the efficiency of the ODS reactions excluding for the oxidation of SCCs with bulky group(s) because of possible steric hindrance [31,154]. Or, the ODS efficiency generally increased with increasing the electron density on S of SCCs [31,154]; however, the efficiency might be decreased by steric effect especially when bulky SCCs or SCCs having alkyl side-chain(s) were oxidized in the presence of porous catalysts.

As mentioned, even though several MOF-based and MOF-derived catalysts (with different metal centers) were applied in ODS reactions, plausible mechanisms for the oxidations were suggested only for some cases. The mentioned mechanisms will be dealt here. Ti-based MOFs (MIL-125-Ti and H_2N-MIL-125-Ti) and their derived carbons have been used as catalysts for ODS reactions [39,104,106,109,111,112,165,167,168]. Moreover, different oxidants, for instance, CHP, TBHP, and H_2O_2 were activated by using Ti-MOFs (and catalysts derived from the MOFs) for successful ODS reactions. For example, the ODS reactions over several Ti-MOFs, in the presence of CHP, might be proceeded by the heterolytic route via the formation of Ti-peroxo species (a coordination complex) that obtained through activation of CHP by the active Ti^{IV} sites of the MOFs [104]). Or, the resulting peroxo species might be responsible for the subsequent peroxidase-like oxidation of DBT to produce DBT sulfoxide, which further oxidized into DBT sulfone via another similar oxidation. Similar to the CHP, TBHP also converted into active Ti-peroxo species (Ti-OOH) via interaction with Ti^{IV} species of MIL-125. The ODS reactions mentioned (with CHP or TBHP) could be carried successfully without using any extractant. However, when H_2O_2 was used as an oxidant in the absence of extractant, the oxidation efficiency was very low (~ 25% DBT

conversion) compared to that with CHP (~ 58% conversion) or TBHP (~98% conversion) after 1 h of reaction [111]. On the other hand, in the presence of MeOH as extractant, H_2O_2 showed the highest activity among the three oxidants. Consequently, it can be assumed that activation of H_2O_2 may be different from that of CHP or TBHP by the MIL-125-Ti (via active Ti-OOH formation). Here, the reactive oxygen free radical species ($\cdot O_2^-$ superoxide radical anion that can oxidize the DBT) might be formed by the interaction between Ti^{IV} and H_2O_2. This mechanism could be assumed from the change of the solution color which is originated from a charge transfer process [111].

In addition, Ti-based catalysts (derived from MOFs), supported on porous carbon, also showed fascinating performance in ODS reactions in the presence of TBHP or H_2O_2 with or without the use of extractant. The studies on ODS over Ti-decorated carbons were mainly focused to suggest the main active component or reason for high activity rather than the exploration of detailed mechanisms [39,165,167,168]. Based on the explanations, it could be assumed that obtained Ti-OOH, from the catalyst having active Ti^{IV} species, might be more effective in ODS than the generated oxygen free radical species [173–175].

Therefore, Ti^{IV} sites of the Ti-based MOFs or MOF-derived catalysts might be suggested as the main active component for the oxidation of SCCs from fuels. Moreover, Ti^{IV} species can activate various oxidant including CHP, TBHP, and H_2O_2 via formation of active Ti-OOH species which then oxidized the SCCs into corresponding sulfoxides or sulfones.

Even though V-based catalysts have been widely used in vapor-phase oxidations [176–178], those were rarely applied in ODS because of the instability or leaching of vanadium species from V-MOFs or V-based catalysts, especially in liquid phase oxidations [106,179]. Therefore, the understanding of the mechanisms for the ODS over the MIL-47-V or MIL-47-V-derived catalysts is very shallow. The ODS reaction over the MIL-47-V was conducted with TBHP as an oxidant in the presence of additional 4-propylphenol. It was suggested that the ODS over MIL-47-V was likely undergoing through heterolytic reaction path by the active V-site on the MOFs rather than the formation of free radical via homolytic cleavage of TBHP, based on the fact that 4-propylphenol, a radical scavenger, does not have any influence on the DBT oxidation [106].

Additionally, the V^{4+} or V^{5+} component was assumed as the main active site for ODS when carbon-supported V-oxides or V-carbides (that derived by the carbonization of MIL-47-V) were used as catalysts in the presence of TBHP [179]. On the other hand, the materials prepared by Kim et al. [179] were composed of V species with different oxidation state (V^{3+}, V^{4+}, V^{5+} and V^{8+}) where changes of the oxidation states were assumed (especially V^{3+} to V^{4+} or V^{5+} and V^{8+} to V^{4+} or V^{5+}) even though V^{4+} and V^{5+} may not undergo in such interchange of oxidation states. Therefore, ODS, in the presence of TBHP, over the carbon-supported V-oxide or V-carbide catalysts may go through a complex route. The reactions possibly processed by the homolytic free radical or heterolytic metal-peroxo [180] or both the free radical and metal-peroxo mechanisms. For a better understanding of the ODS mechanism over the V-oxides- or V-carbides-supported on carbon, more studies are required.

MOFs having Zr metal centers (pristine or defecated and post functionalized ones) were also found to be highly active catalysts for ODS reactions via activation of an oxidant. The Zr^{IV}-OH species of the Zr-oxo-cluster of Zr-MOFs (e. g. UiO-66-Zr) may lead to the formation of Zr^{IV}–peroxo groups (Zr-OOH) by the interaction with H_2O_2 by a heterolytic process, in accordance with the previous reports [181–183]. The active oxygen atom of the Zr^{IV}–peroxo groups then attacked the sulfur atom of the substrates; and, SCCs converted into respective sulfoxides (and finally sulfoxides into sulfones). However, some reports proposed the formation of active $\cdot OH$ free radical via homolytic process, by the interaction of $Zr-OH(OH_2)$ (of Zr-MOF) with H_2O_2, which promotes the oxidation reactions. Very recently, based on the experimental observation for the oxidation of DBT over MOF-808-Zr, Zheng et al. [118] proposed a plausible mechanism (Scheme 1a) or oxidations via formation of $\cdot OH$ and $\cdot O_2^-$ free radicals. The detailed mechanism
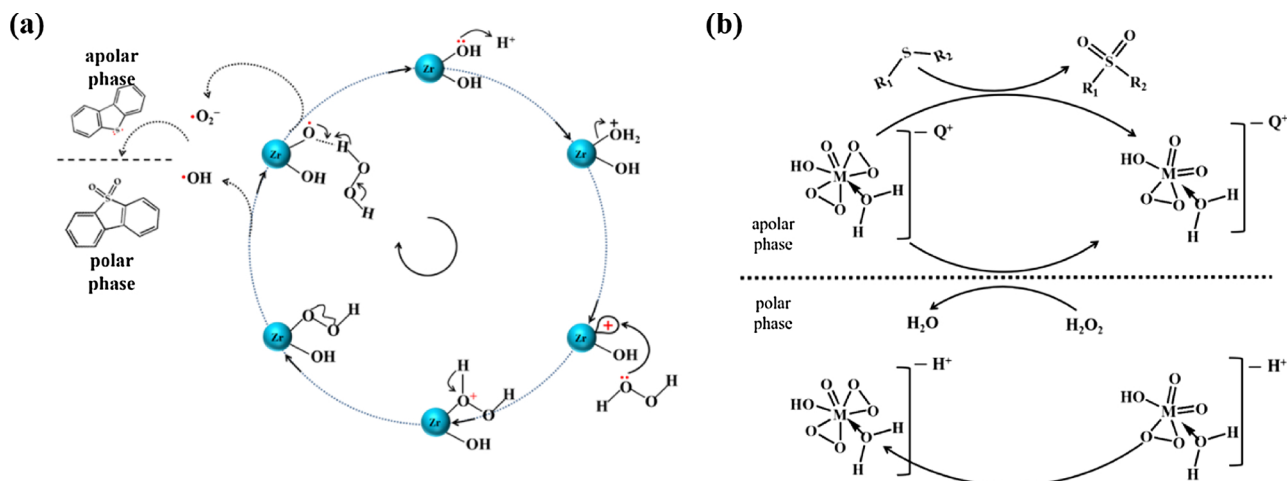
Scheme 1. (a) Homolysis and (b) heterolysis of peroxides, and plausible ODS mechanisms in biphasic reaction media (Adapted/reproduced from Ref. [118,172], Copyright 2019 ACS and Elsevier).

includes seven steps: (i) the protonation of Zr-$(OH)_2$ sites to form Zr-OH (OH_2^+) which (ii) undergo dehydration to form unsaturated Zr sites. (iii) the oxidant (H_2O_2) attacked the unsaturated Zr-sites (serving as Lewis acid) which (iv) generate Zr-OOH complexes; (v) peroxometallic complex undergo $O-O$ bond cleavage leading to the formation of •OH radicals and (vi) the Zr-O• and H_2O_2 reacted each other to result in •O_2^- radicals (vii) both the radicals (•OH and •O_2^-) oxidized DBT into the corresponding sulfoxide or sulfone. Chen et al. [61] also suggested a very similar mechanism via thorough analysis of the properties of the catalyst and ODS reaction in the presence of TBHP using MoO_2/g-boron nitride as the catalyst. Therefore, Zr-MOFs having defect-sites (or, unsaturated sites) can be suggested as a good catalyst for ODS (via activation of H_2O_2) by the formation of Zr-OOH groups or •OH and •O_2^- free radicals.

Furthermore, the ODS using H_2O_2 over H_2N-TMU-53-Co was not affected even after addition of excess scavengers such as isopropanol and p-benzoquinone [114]. The observed results suggested that the ODS over NH_2-TMU-53-Co may not be preceded via expected homolytic formation of active •OH or •O_2^- free radicals. Consequently, the oxidation of DBT might be resulted by the direct catalysis by NH_2-TMU-53-Co rather than the formation of any free radicals. Further work is required to understand the ODS mechanism with the Co-based catalysts.

Cr-based MOFs rarely showed their efficacy in ODS. However, Gómez-Paricio et al [115] nicely demonstrated the activity of a Cr-MOF (MIL-101-Cr) in ODS under aerobic condition. Based on the observed results over the MIL-101-Cr under molecular oxygen, as expected, radical chain auto-oxidation mechanism (Scheme 2) was suggested [184,185]. In this mechanism, during the initiation of the oxidation, •DBT^+ and •O_2^- could be formed and a chain of propagation occurs by reaction with molecular oxygen to form •DBT-O_2^+ which abstracted electron from the neutral DBT thereby resulted in the DBT-O_2 (sulfone) as a final product with another •DBT^+ radical. The interaction between the Cr^{3+} with molecular O_2 may lead to the formation of some reactive oxygen species that generated the first •DBT^+ radical for a cyclic auto-oxidation process. These assumptions were supported by the highly reduced oxidation efficiency in the presence of a radical scavenger (2,2,6,6-tetramethyl-1-piperidinyloxy) and EPR and Raman spectroscopic analyses.

On the other hand, POMs or HPAs are widely used in oxidation reaction via activation of various oxidants by the formation of metal-peroxo active species [172,186]. However, because of the high solubility of POMs, recently they were incorporated into a variety of porous structures, especially into MOFs having well-defined structures with tunable pore architectures to find stable POM-based catalysts for liquid-phase oxidation reactions. Generally, SCCs in the non-polar oil phase

was initially diffused into the polar (e. g. acetonitrile) phase, then the POM-encapsulated MOF catalysts adsorbed the DBT and H_2O_2 into their pores. Some of the adsorbed H_2O_2 could readily interact with the loaded POM to form metal-peroxo species by the heterolytic process (such as W(VI) − peroxo) which then oxidize the SCCs into respective sulfones/sulfoxides. In addition, along with an active site from POM for ODS, the metal center of the used MOF also may have a role in the efficiency and mechanism for the ODS reactions. For example, Lin et al [150] demonstrated the possible role of the central metals from both the POM (PTA was used as a precursor for POM) and MOF in the oxidation of DBT using a Zr-MOF (MOF-808A-Zr) loaded with POM. As suggested, the W center of PTA oxidized the DBT through W(VI)-peroxo formation; however, H_2O_2 can be also decomposed to active •OH by Zr − $OH(OH_2)$ on the Zr-oxo-clusters of MOF-808A-Zr. Moreover, a very recent observation on the ODS reaction using PMA@UiO-66-Zr, in the presence of radical scavenger, demonstrated that the oxidation reactions proceeded via formation of •OH by the Mo^{5+} of the PMA [149]. Therefore, the cooperative role of POM and metal nodes of the MOFs (the metal should be able to activate the oxidant) may contribute to the high reactivity as well as the oxidation mechanisms over the POM@MOF based catalysts.

Till now, the exploration of ODN reaction mechanism is very primitive compared to the studies on the mechanisms for ODS. The chemical properties, as well as the reactivity of the smaller N atom (a second row and group XV element) in heterocyclic NCCs are different from those of the S atom (a third row and group XVI element). Therefore, the mechanisms for ODN might be different from that of the
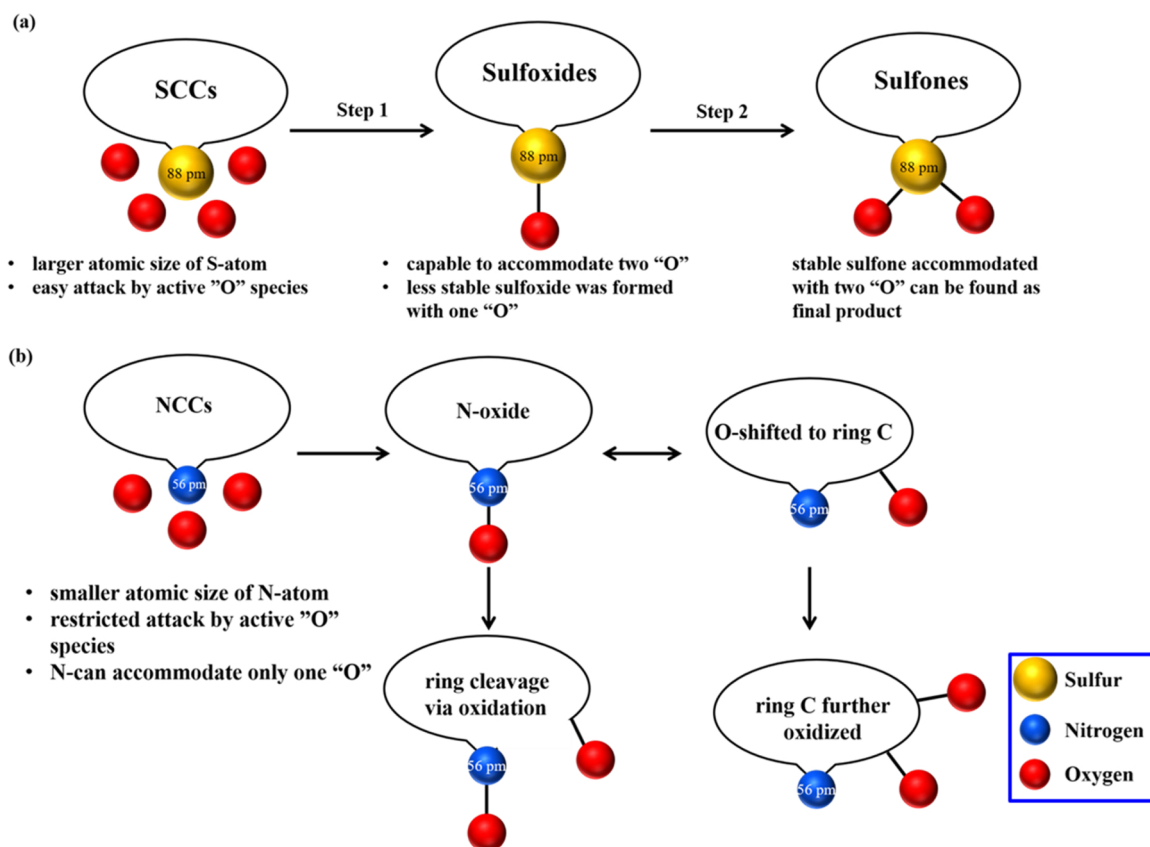
(a) Initiation
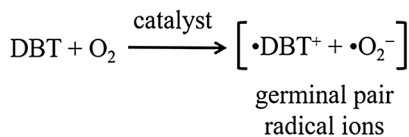
(b) Radical chain propagation
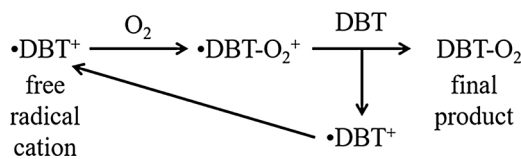
Scheme 2. Proposed chain auto-oxidation mechanism for ODS with molecular oxygen (Adapted from Ref. [115], Copyright 2016 Royel Society of Chemistry).

Scheme 3. Representation of oxidation paths for (a) SCCs and (b) NCCs.

ODS which is required to have much attention to explore.

Bhadra et al [50] studied oxidative removal of IND (and several IND-derivatives such as 1Me-IND, 2Me-IND, and 3Me-IND), PRL, CBZ (as non-basic NCCs), and QUI (as basic NCC). In that study, MDC-C, H_2O_2, and CH_3COOH were applied as the catalyst, oxidant, and extractant, respectively. MDC-C was a TiO_2-decorated carbon catalyst, derived from a composite MOF (ZIF-8-Zn@H2**N**-MIL-125-Ti). Considering the observed ODN efficiency in terms of conversion and kinetics (in an order of IND > 2Me-IND > 3Me-IND > 1Me-IND > PRL > CBZ) (Fig. 17b), it could be assumed that the oxidation activities of NCCs are different from one another and possibly are dependent on their chemical properties. To understand the mechanism, the electron density of the N-atom on the studied NCCs were estimated by the Mulliken population method, and the results were shown to have the order CBZ > IND > 2Me-IND > 3Me-IND > 1Me-IND > PRL > QUI (Table 1). From the orders of ODN efficiency and electron density, it was suggested that the activity generally increased with increasing electron density on the N atom of the tested NCCs (except CBZ), quite similar to the ODS of SCCs. Therefore, ODN might also be explained by the electron density of the heteroatom (N atom) on the NCCs (especially INDs), similar to the ODS [30,31,57,165,187–191]. Or, the electrophilic addition of an active oxygen atom onto the substrates (via N on the ONCs) might be very important in the ODN, similar to the ODS of SCCs [40,154]. However, it should be emphasized that the oxidizing positions (in ODN and ODS) are quite different from each other. For example, the oxidation of ODN occurs at carbon atom(s) (C_2 or C_3) of NCCs, whereas the S atom oxidized to sulfone (or sulfoxide) in ODS of SCCs. This might be related to the mentioned differences between S and N. Importantly, larger S atom of the SCCs can efficiently accommodate maximum two oxygen atoms during the oxidation process; therefore, oxidation may occur on the S atom and resulted in corresponding sulfones as a stable final product (Scheme 3a). On the contrary, smaller N atom (that can accept only one oxygen atom) in NCCs might be firstly

oxidized into N-O (or N-O xide) species; however, the obtained oxygenated N species, even formed, might be transformed into more stable species and might lead to the shifting of O atom onto nearby ring carbon atoms. Moreover, depending on the properties of the NCCs and reaction condition, sometimes, the final product might be a mixture of usual oxidized product and ring-cleavage product or only the cleavage product (oxygenated NCCs), accompanied by the cleavage of C-N bonds of the heterocyclic ring of the NCCs [50,192]. The plausible mechanism is shown as Scheme 3b. Finally, further work is required to understand the ODN mechanism including the role of the electron density on N (even though the N atom is not oxidized or attacked eventually in ODN) and effect of basicity or aromaticity of NCCs on oxidation.

5. Summary and outlook

A wide variety of MOFs, including pristine and functionalized ones, and MOF-derived materials were found as promising catalysts for oxidative purification of fuel including ODS. Following conclusions or summaries can be drawn from the studies on the ODS/ODN over MOF-based and MOF-derived catalysts.

(i) Pristine MOFs composed of Ti-, V-, Co-, Zr-, Cr-, and Fe-ions have shown high efficiency in ODS catalysis. The performances of MOFs may vary depending on the physicochemical properties including constituent active metal-center, porosity, window/pore size, along with the studied reaction conditions.

(ii) The performances of MOFs for ODS can be boosted up via creating defect sites or increasing the open metal sites on its structures. The amount or number of defect sites can be tuned via developing suitable synthetic methods or post-modification of the MOFs.

(iii) Incorporation of active species (especially, POM/HPA or IL) is another way to increase the ODS capability of MOFs. Both in-situ and post-encapsulations of active components into the accessible

pores of MOFs were found as effective modification method to develop new ODS catalysts.

(iv) Several MOFs (pristine, composite, bimetallic and active species-loaded ones) can be used as precursors to prepare efficient ODS/ODN catalysts. The performances were generally dependent on the porosity, size and distribution and crystal phases of the active nanoparticles.

(v) The mechanisms for ODS might be mainly dependent on the active metal center of the used catalysts; however, sometimes types of oxidants also play some roles on the mechanisms for ODS. ODS using peroxides, proceeded two probable paths via formation of active free radicals or metal-peroxo species by homolytic or heterolytic cleavage, respectively, of the oxidant. Chain auto-oxidation was generally suggested when molecular oxygen was used as an oxidant.

(vi) Electron density of S or N was very important, suggesting the electrophilic addition of active oxygen atom onto S or N. However, oxidized N, even if obtained, might transfer oxygen onto nearby carbon of NCCs, different from the oxidized S (which is explainable with the relatively small size of N).

(vii) Finally, it can be concluded that MOF-based and MOF-derived catalysts are very promising for ODS/ODN of fuel.

Moreover, prospects or new research fields on ODS/ODN might be suggested as follows:

(i) Even though the ODS (and ODN) studies showed the possibility of development, there has been a shallow understanding of the reaction mechanism, so far. Therefore, mechanistic studies, especially with in-situ analyses (EPR, NMR, FTIR, etc.), are required to understand the contributions of central metal ions, oxidants, and extractants.

(ii) Theoretical calculations will be also required in order to understand the active species or intermediates of oxidation (and relative stability of intermediates or transition states).

(iii) Even though possible purification of fuel with ODS/ODN was suggested, studies in more realistic conditions (from real fuel, under relatively low oxidant/S ratio, recycle of catalysts and so on) are required for possible applications including compensating studied/developed technologies.

(iv) There have been results that are not agreeable one another (for example, the importance of perfect MOF and defected MOF) or that require further confirmation (such as extremely low activation energy). More precise experiments (including round-robin ones) are required in order to suggest a meaningful or reliable approach or development.

(v) Addition to the developed methods (in-situ or post-loading of active species into MOFs) for modification of conventional MOFs, use of the functionalities of MOFs, especially, unsaturated metal active sites to form more stable composites (e. g. POM@MOF) via chemical interactions might be sought as an alternative approach to prepare stable and efficient catalysts for ODS/ODN reaction.

(vi) Commercialization of a catalyst depends mainly on economics; however, MOFs or MOF-derived materials are generally expensive compared with simple inorganic materials such as oxides and polyoxometalates. Therefore, researches to reduce the cost for preparation and modification of new catalysts will be required for practical applications.

(vii) Finally, the application of ODS/ODN might be considered including complementary cooperation with hydropurification (for example, hydrogenation and subsequent oxidation of stubborn substrates for fuel cell applications, etc.), rather than the replacement of existing technology.

Declaration of Competing Interest

The authors declare that they have no known competing financial interests or personal relationships that could have appeared to influence the work reported in this paper.

Acknowledgments

References

[1] J. Chow, R.J. Kopp, P.R. Portney, Energy resources and global development, Science 302 (2003) 1528–1531.

[2] N.L. Panwar, S.C. Kaushik, S. Kothari, Role of renewable energy sources in environmental protection: a review, Renew. Sustain. Energy Rev. 15 (2011) 1513–1524.

[3] S. Kumar, H.T. Kwon, K.H. Choi, W. Lim, J.H. Cho, K. Tak, I. Moon, LNG: an eco-friendly cryogenic fuel for sustainable development, Appl. Energy 88 (2011) 4264–4273.

[4] N. Li, X.L. Ma, Q.F. Zha, C.S. Song, Analysis and comparison of nitrogen compounds in different liquid hydrocarbon streams derived from petroleum and coal, Energy Fuels 24 (2010) 5539–5547.

[5] G.H. Prado, Y. Rao, A. de Klerk, Nitrogen removal from oil: a review, Energy Fuels 31 (2016) 14–36.

[6] B. Pawelec, R.M. Navarro, J.M. Campos-Martin, J.L. Fierro, Towards near zero-sulfur liquid fuels: a perspective review, Catal. Sci. Technol. 3 (2013) 3376-3376.

[7] A.M. Liaquat, M.A. Kalam, H.H. Masjuki, M.H. Jayed, Potential emissions reduction in road transport sector using biofuel in developing countries, Atmos. Environ. 44 (2010) 3869–3877.

[8] Y.Q. Jin, L. Lu, X.J. Ma, H.M. Liu, Y. Chi, K. Yoshikawa, Effects of blending hydrothermally treated municipal solid waste with coal on co-combustion characteristics in a lab-scale fluidized bed reactor, Appl. Energy 102 (2013) 563–570.

[9] R. Colvile, E. Hutchinson, J. Mindell, R. Warren, The transport sector as a source of air pollution, Atmos. Environ. 35 (2001) 1537–1565.

[10] A. Stanislaus, A. Marafi, M.S. Rana, Recent advances in the science and technology of ultra low sulfur diesel (ULSD) production, Catal. Today 153 (2010) 1–68.

[11] P.S. Kulkarni, C.A. Afonso, Deep desulfurization of diesel fuel using ionic liquids: current status and future challenges, Green Chem. 12 (2010) 1139–1149.

[12] N. Li, X. Ma, Q. Zha, C. Song, Analysis and comparison of nitrogen compounds in different liquid hydrocarbon streams derived from petroleum and coal, Energy Fuels 24 (2010) 5539–5547.

[13] G.C. Laredo, P.M. Vega-Merino, F. Trejo-Zarraga, J. Castillo, Denitrogenation of middle distillates using adsorbent materials towards ULSD production: a review, Fuel Process. Technol. 106 (2013) 21–32.

[14] H. Zhang, G. Li, Y.H. Jia, H.O. Liu, Adsorptive removal of nitrogen-containing compounds from fuel, J. Chem. Eng. Data 55 (2010) 173–177.

[15] I. Ahmed, S.H. Jhung, Adsorptive desulfurization and denitrogenation using metal-organic frameworks, J. Hazard. Mater. 301 (2016) 259–276.

[16] O. González-García, L. Cedeño-Caero, V-Mo based catalysts for oxidative desulfurization of diesel fuel, Catal. Today 148 (2009) 42–48.

[17] P.G. Duan, P.E. Savage, Catalytic hydrothermal hydrodenitrogenation of pyridine, Appl. Catal. B 108 (2011) 54–60.

[18] C.S. Raghuveer, J.W. Thybaut, G.B. Marin, Pyridine hydrodenitrogenation kinetics over a sulphided NiMo/gamma-Al$_2$O$_3$ catalyst, Fuel 171 (2016) 253–262.

[19] H.Y. Yao, G. Wang, C.C. Zuo, C.S. Li, E.Q. Wang, S.J. Zhang, Deep hydro-denitrification of pyridine by solid catalyst coupling with ionic liquids under mild conditions, Green Chem. 19 (2017) 1692–1700.

[20] G.H.C. Prado, Y. Rao, A. de Klerk, Nitrogen removal from oil: a review, Energy Fuels 31 (2017) 14–36.

[21] J.M. Campos-Martin, M.C. Capel-Sanchez, P. Perez-Presas, J. Fierro, Oxidative processes of desulfurization of liquid fuels, J. Chem. Technol. Biotechnol. 85 (2010) 879–890.

[22] J.M. Foght, Whole-cell bio-processing of aromatic compounds in crude oil and fuels, Stud. Surf. Sci. Catal. Elsevier, 2004, pp. 145–175.

[23] I. Babich, J. Moulijn, Science and technology of novel processes for deep desulfurization of oil refinery streams: a review, Fuel 82 (2003) 607–631.

[24] X.C. Chen, S. Yuan, A.A. Abdeltawab, S.S. Al-Deyab, J.W. Zhang, L. Yu, G.R. Yu, Extractive desulfurization and denitrogenation of fuels using functional acidic ionic liquids, Sep. Purif. Technol. 133 (2014) 187–193.

[25] R. Abro, M. Abro, S.R. Gao, A.W. Bhutto, Z.M. Ali, A. Shah, X.C. Chen, G.R. Yu, Extractive denitrogenation of fuel oils using ionic liquids: a review, RSC Adv. 6 (2016) 93932–93946.

[26] I. Ahmed, S.H. Jhung, Composites of metal–organic frameworks: preparation and application in adsorption, Mater. Today 17 (2014) 136–146.

[27] N.A. Khan, S.H. Jhung, Adsorptive removal and separation of chemicals with metal-organic frameworks: Contribution of π-complexation, J. Hazard. Mater. 325 (2017) 198–213.

[28] N.A. Khan, Z. Hasan, S.H. Jhung, Adsorption and removal of sulfur or nitrogen-containing compounds with metal-organic frameworks (MOFs), Adv. Porous Mater. 1 (2013) 91–102.

[29] P. Tan, Y. Jiang, L.-B. Sun, X.-Q. Liu, K. AlBahily, U. Ravon, A. Vinu, Design and fabrication of nanoporous adsorbents for the removal of aromatic sulfur compounds, J. Mater. Chem. A 6 (2018) 23978–24012.

[30] M.H. Ibrahim, M. Hayyan, M.A. Hashim, A. Hayyan, The role of ionic liquids in desulfurization of fuels: a review, Renew. Sustain. Energy Rev. 76 (2017) 1534–1549.

[31] S.N. Wei, H.J. He, Y. Cheng, C.P. Yang, G.M. Zeng, L. Qiu, Performances, kinetics and mechanisms of catalytic oxidative desulfurization from oils, RSC Adv. 6 (2016) 103253–103269.

[32] H. Zhao, G.A. Baker, Oxidative desulfurization of fuels using ionic liquids: a review, Front. Chem. Sci. Eng. 9 (2015) 262–279.

[33] H. Shang, H. Zhang, W. Du, Z. Liu, Development of microwave assisted oxidative desulfurization of petroleum oils: a review, J. Ind. Eng. Chem. 19 (2013) 1426–1432.

[34] A.W. Bhutto, R. Abro, S. Gao, T. Abbas, X. Chen, G. Yu, Oxidative desulfurization of fuel oils using ionic liquids: a review, J. Taiwan Inst. Chem. Eng. 62 (2016) 84–97.

[35] M. Ja'fari, S.L. Ebrahimi, M.R. Khosravi-Nikou, Ultrasound-assisted oxidative desulfurization and denitrogenation of liquid hydrocarbon fuels: a critical review, Ultrason. Sonochem. 40 (2018) 955–968.

[36] A.E.S. Choi, S. Roces, N. Dugos, M.-W. Wan, Oxidation by H_2O_2 of bezothiophene and dibenzothiophene over different polyoxometalate catalysts in the frame of ultrasound and mixing assisted oxidative desulfurization, Fuel 180 (2016) 127–136.

[37] M. Zhu, G. Luo, L. Kang, B. Dai, Novel catalyst by immobilizing a phosphotungstic acid on polymer brushes and its application in oxidative desulfurization, RSC Adv. 4 (2014) 16769–16776.

[38] Y. Qin, S. Xun, L. Zhan, Q. Lu, M. He, W. Jiang, H. Li, M. Zhang, W. Zhu, H. Li, Synthesis of mesoporous WO_3/TiO_2 catalyst and its excellent catalytic performance for the oxidation of dibenzothiophene, New J. Chem. 41 (2017) 569–578.

[39] M. Sarker, B.N. Bhadra, S. Shin, S.H. Jhung, TiO2-integrated carbon prepared via pyrolysis of Ti-loaded metal–organic frameworks for redox catalysis, ACS Appl. Nano Mater. 2 (2019) 191–201.

[40] Z. Hasan, J. Jeon, S.H. Jhung, Oxidative desulfurization of benzothiophene and thiophene with WO_x/ZrO_2 catalysts: effect of calcination temperature of catalysts, J. Hazard. Mater. 205 (2012) 216–221.

[41] Y. Shiraishi, K. Tachibana, T. Hirai, I. Komasawa, A novel desulfurization process for fuel oils based on the formation and subsequent precipitation of S-alkylsulfonium salts. 3. Denitrogenation behavior of light oil feedstocks, Ind. Eng. Chem. Res. 40 (2001) 3390–3397.

[42] D. Carnaroglio, E.C. Gaudino, S. Mantegna, E.M. Moreira, A.V. de Castro, E.M.M. Flores, G. Cravotto, Ultrasound-assisted oxidative desulfurization/denitrification of liquid fuels with solid oxidants, Energy Fuels 28 (2014) 1854–1859.

[43] Z. Hu, H.L. Yu, Ultrasound assisted oxidative denitrification of diesel by formic acid/hydrogen peroxide, Pet. Sci. Technol. 34 (2016) 268–273.

[44] A. Ishihara, D.H. Wang, F. Dumeignil, H. Amano, E.W.H. Qian, T. Kabe, Oxidative desulfurization and denitrogenation of a light gas oil using an oxidation/adsorption continuous flow process, Appl. Catal. A 279 (2005) 279–287.

[45] X. Zhou, H. Ma, X. Fu, C. Yao, J. Xiao, Catalytic oxidation of carbazole using t-butyl hydroperoxide over molybdenum catalysts, J. Fuel Chem. Technol. 38 (2010) 75–79.

[46] Z. Hu, H. Yu, Oxidative denitrification of diesel by phosphomolybdic acid/hydrogen peroxide, Pet. Sci. Technol. 33 (2015) 968–974.

[47] A.S. Ogunlaja, O.S. Alade, Catalysed oxidation of quinoline in model fuel and the selective extraction of quinoline-N-oxide with imidazoline-based ionic liquids, Egypt. J. Pet. 27 (2018) 159–168.

[48] A.S. Ogunlaja, M.S. Abdul-quadir, P.E. Kleyi, E.E. Ferg, P. Watts, Z.R. Tshentu, Towards oxidative denitrogenation of fuel oils: vanadium oxide-catalysed oxidation of quinoline and adsorptive removal of quinoline-N-oxide using 2,6-pyridine-polybenzimidazole nanofibers, Arabian J. Chem. 12 (2019) 198–214.

[49] J. Huang, X. Zhang, H. Song, C. Chen, F. Han, C. Wen, Protonated graphitic carbon nitride coated metal-organic frameworks with enhanced visible-light photocatalytic activity for contaminants degradation, Appl. Surf. Sci. 441 (2018) 85–98.

[50] B.N. Bhadra, J.Y. Song, N. Uddin, N.A. Khan, S. Kim, C.H. Choi, S.H. Jhung, Oxidative denitrogenation with TiO2@porous carbon catalyst for purification of fuel: chemical aspects, Appl. Catal. B 240 (2019) 215–224.

[51] H. Ji, J. Sun, P. Wu, Y. Wu, J. He, Y. Chao, W. Zhu, H. Li, Silicotungstic acid immobilized on lamellar hexagonal boron nitride for oxidative desulfurization of fuel components, Fuel 213 (2018) 12–21.

[52] J.F. Palomeque-Santiago, R. López-Medina, R. Oviedo-Roa, J. Navarrete-Bolaños, R. Mora-Vallejo, J.A. Montoya-de la Fuente, J.M. Martínez-Magadán, Deep oxidative desulfurization with simultaneous oxidative denitrogenation of diesel fuel and straight run gas oil, Appl. Catal. B 236 (2018) 326–337.

[53] N.A. Khan, B.N. Bhadra, S.W. Park, Y.-S. Han, S.H. Jhung, Tungsten nitride, well-dispersed on porous carbon: remarkable catalyst, produced without addition of ammonia, for the oxidative desulfurization of liquid fuel, Small (2019) 1901564.

[54] B.N. Bhadra, N.A. Khan, S.H. Jhung, Co supported on N-doped carbon, derived from bimetallic azolate framework-6: a highly effective oxidative desulfurization catalyst, J. Mater. Chem. A 7 (2019) 17823–17833, https://doi.org/10.1039/C1039TA03613J.

[55] K. Chen, N. Liu, M. Zhang, D. Wang, Oxidative desulfurization of dibenzothiophene over monoclinic VO_2 phase-transition catalysts, Appl. Catal. B 212 (2017) 32–40.

[56] H. Gómez-Bernal, L. Cedeño-Caero, A. Gutiérrez-Alejandre, Liquid phase oxidation of dibenzothiophene with alumina-supported vanadium oxide catalysts: an alternative to deep desulfurization of diesel, Catal. Today 142 (2009) 227–233.

[57] C. Shen, Y.J. Wang, J.H. Xu, G.S. Luo, Oxidative desulfurization of DBT with H_2O_2 catalysed by TiO_2/porous glass, Green Chem. 18 (2016) 771–781.

[58] C. Shen, Y.J. Wang, J.H. Xu, G.S. Luo, Synthesis of TS-1 on porous glass beads for catalytic oxidative desulfurization, Chem. Eng. J. 259 (2015) 552–561.

[59] E. Lorençon, D.C.B. Alves, K. Krambrock, E.S. Ávila, R.R. Resende, A.S. Ferlauto, R.M. Lago, Oxidative desulfurization of dibenzothiophene over titanate nanotubes, Fuel 132 (2014) 53–61.

[60] X. Yao, C. Wang, H. Liu, H. Li, P. Wu, L. Fan, H. Li, W. Zhu, Immobilizing highly catalytically molybdenum oxide nanoparticles on graphene-analogous BN: stable heterogeneous catalysts with enhanced aerobic oxidative desulfurization performance, Ind. Eng. Chem. Res. 58 (2018) 863–871.

[61] K. Chen, X.-M. Zhang, X.-F. Yang, M.-G. Jiao, Z. Zhou, M.-H. Zhang, D.-H. Wang, X.-H. Bu, Electronic structure of heterojunction $MoO_2/g-C_3N_4$ catalyst for oxidative desulfurization, Appl. Catal. B 238 (2018) 263–273.

[62] P. Wu, W. Zhu, B. Dai, Y. Chao, C. Li, H. Li, M. Zhang, W. Jiang, H. Li, Copper nanoparticles advance electron mobility of graphene-like boron nitride for enhanced aerobic oxidative desulfurization, Chem. Eng. J. 301 (2016) 123–131.

[63] L. Lu, J. He, P. Wu, Y. Wu, Y. Chao, H. Li, D. Tao, L. Fan, H. Li, W. Zhu, Taming electronic properties of boron nitride nanosheets as metal-free catalysts for aerobic oxidative desulfurization of fuels, Green Chem. 20 (2018) 4453–4460.

[64] Q. Gu, G. Wen, Y. Ding, K.-H. Wu, C. Chen, D. Su, Reduced graphene oxide: a metal-free catalyst for aerobic oxidative desulfurization, Green Chem. 19 (2017) 1175–1181.

[65] J. He, P. Wu, L. Lu, H. Sun, Q. Jia, M.-Q. Hua, M. He, C. Xu, W. Zhu, H.-m. Li, Synthesis of N, O-doped porous graphene from petroleum coke for deep oxidative desulfurization of fuel, Energy Fuels (2019).

[66] Q. Jia, J. He, P. Wu, J. Luo, Y. Wei, H. Li, S. Xun, W. Zhu, H. Li, Tuning interfacial electronic properties of carbon nitride as an efficient catalyst for ultra-deep oxidative desulfurization of fuels, Mol. Catal. 468 (2019) 100–108.

[67] H. Furukawa, K.E. Cordova, M. O'Keeffe, O.M. Yaghi, The chemistry and applications of metal-organic frameworks, Science 341 (2013) 1230444.

[68] A.J. Howarth, Y. Liu, P. Li, Z. Li, T.C. Wang, J.T. Hupp, O.K. Farha, Chemical, thermal and mechanical stabilities of metal–organic frameworks, Nat. Rev. Mater. 1 (2016) 15018.

[69] A.J. Howarth, A.W. Peters, N.A. Vermeulen, T.C. Wang, J.T. Hupp, O.K. Farha, Best practices for the synthesis, activation, and characterization of metal–organic frameworks, Chem. Mater. 29 (2016) 26–39.

[70] T. Islamoglu, S. Goswami, Z. Li, A.J. Howarth, O.K. Farha, J.T. Hupp, Postsynthetic tuning of metal–organic frameworks for targeted applications, Acc. Chem. Res. 50 (2017) 805–813.

[71] Z. Hasan, S.H. Jhung, Removal of hazardous organics from water using metal-organic frameworks (MOFs): plausible mechanisms for selective adsorptions, J. Hazard. Mater. 283 (2015) 329–339.

[72] S.H. Jhung, N.A. Khan, Z. Hasan, Analogous porous metal–organic frameworks: synthesis, stability and application in adsorption, CrystEngComm 14 (2012) 7099–7109.

[73] L. Zhu, X.-Q. Liu, H.-L. Jiang, L.-B. Sun, Metal–organic frameworks for heterogeneous basic catalysis, Chem. Rev. 117 (2017) 8129–8176.

[74] S.L. Anderson, K.C. Stylianou, Biologically derived metal organic frameworks, Coord. Chem. Rev. 349 (2017) 102–128.

[75] C. Wang, X. Liu, N.K. Demir, J.P. Chen, K. Li, Applications of water stable metal-organic frameworks, Chem. Soc. Rev. 45 (2016) 5107–5134.

[76] J. Jiang, O.M. Yaghi, Brønsted acidity in metal–organic frameworks, Chem. Rev. 115 (2015) 6966–6997.

[77] A. Schoedel, M. Li, D. Li, M. O'Keeffe, O.M. Yaghi, Structures of metal–organic frameworks with rod secondary building units, Chem. Rev. 116 (2016) 12466–12535.

[78] P. Horcajada, R. Gref, T. Baati, P.K. Allan, G. Maurin, P. Couvreur, G. Ferey, R.E. Morris, C. Serre, Metal–organic frameworks in biomedicine, Chem. Rev. 112 (2011) 1232–1268.

[79] S. Yuan, L. Feng, K. Wang, J. Pang, M. Bosch, C. Lollar, Y. Sun, J. Qin, X. Yang, P. Zhang, Stable metal–organic frameworks: design, synthesis, and applications, Adv. Mater. (2018) 1704303.

[80] H. Assi, G. Mouchaham, N. Steunou, T. Devic, C. Serre, Titanium coordination compounds: from discrete metal complexes to metal–organic frameworks, Chem. Soc. Rev. 46 (2017) 3431–3452.

[81] R. Sakamoto, Bottom-up creation of functional low-dimensional materials based on metal complexes, Bull. Chem. Soc. Jpn. 90 (2016) 272–278.

[82] Y.G. Huang, S.Q. Wu, W.H. Deng, G. Xu, F.L. Hu, J.P. Hill, W. Wei, S.Q. Su, L.K. Shrestha, O. Sato, Selective CO_2 capture and high proton conductivity of a functional star-of-david catenane metal–organic framework, Adv. Mater. 29 (2017) 1703301.

[83] Y.-G. Huang, Y. Shiota, M.-Y. Wu, S.-Q. Su, Z.-S. Yao, S. Kang, S. Kanegawa, G.-L. Li, S.-Q. Wu, T. Kamachi, Superior thermoelasticity and shape-memory nanopores in a porous supramolecular organic framework, Nat. Commun. 7 (2016) 11564.

[84] J. Li, X. Wang, G. Zhao, C. Chen, Z. Chai, A. Alsaedi, T. Hayat, X. Wang, Metal–organic framework-based materials: superior adsorbents for the capture of toxic and radioactive metal ions, Chem. Soc. Rev. 47 (2018) 2322–2356.

[85] G.-J. Ren, Y.-Q. Liu, T.-L. Hu, X.-H. Bu, Two robust metal–organic frameworks with uncoordinated N atoms for CO_2 adsorption, CrystEngComm 17 (2015) 8198–8201.

[86] N. Li, R. Feng, J. Zhu, Z. Chang, X.-H. Bu, Conformation versatility of ligands in

coordination polymers: from structural diversity to properties and applications, Coord. Chem. Rev. (2018).

[87] H. Wang, Q.-L. Zhu, R. Zou, Q. Xu, Metal-organic frameworks for energy applications, Chem 2 (2017) 52–80.

[88] V. Malgras, Q. Ji, Y. Kamachi, T. Mori, F.-K. Shieh, K.C.-W. Wu, K. Ariga, Y. Yamauchi, Templated synthesis for nanoarchitectured porous materials, Bull. Chem. Soc. Jpn. 88 (2015) 1171–1200.

[89] K.J. Lee, J.H. Lee, S. Jeoung, H.R. Moon, Transformation of metal–organic frameworks/coordination polymers into functional nanostructured materials: experimental approaches based on mechanistic insights, Acc. Chem. Res. 50 (2017) 2684–2692.

[90] L. Kong, J. Zhu, W. Shuang, X.H. Bu, Nitrogen-doped wrinkled carbon foils derived from MOF nanosheets for superior sodium storage, Adv. Energy Mater. (2018) 1801515.

[91] B. Liu, H. Shioyama, T. Akita, Q. Xu, Metal-organic framework as a template for porous carbon synthesis, J. Am. Chem. Soc. 130 (2008) 5390–5391.

[92] G. Xu, P. Nie, H. Dou, B. Ding, L. Li, X. Zhang, Exploring metal organic frameworks for energy storage in batteries and supercapacitors, Mater. Today 20 (2017) 191–209.

[93] B.Y. Guan, X.Y. Yu, H.B. Wu, X.W.D. Lou, Complex nanostructures from materials based on metal–organic frameworks for electrochemical energy storage and conversion, Adv. Mater. 29 (2017) 1703614.

[94] W. Xia, A. Mahmood, R. Zou, Q. Xu, Metal–organic frameworks and their derived nanostructures for electrochemical energy storage and conversion, Energy Environ. Sci. 8 (2015) 1837–1866.

[95] Y.V. Kaneti, J. Tang, R.R. Salunkhe, X. Jiang, A. Yu, K.C.W. Wu, Y. Yamauchi, Nanoarchitectured design of porous materials and nanocomposites from metal-organic frameworks, Adv. Mater. 29 (2017) 1604898.

[96] W. Chaikittisilp, K. Ariga, Y. Yamauchi, A new family of carbon materials: synthesis of MOF-derived nanoporous carbons and their promising applications, J. Mater. Chem. A 1 (2013) 14–19.

[97] R.R. Salunkhe, Y. Kamachi, N.L. Torad, S.M. Hwang, Z. Sun, S.X. Dou, J.H. Kim, Y. Yamauchi, Fabrication of symmetric supercapacitors based on MOF-derived nanoporous carbons, J. Mater. Chem. A 2 (2014) 19848–19854.

[98] B.N. Bhadra, S.H. Jhung, Well-dispersed Ni or MnO nanoparticles on mesoporous carbons: preparation via carbonization of bimetallic MOF-74s for highly reactive redox catalysts, Nanoscale 10 (2018) 15035–15047.

[99] K. Shen, X. Chen, J. Chen, Y. Li, Development of MOF-derived carbon-based nanomaterials for efficient catalysis, ACS Catal. 6 (2016) 5887–5903.

[100] S.-N. Zhao, X.-Z. Song, S.-Y. Song, H.-j. Zhang, Highly efficient heterogeneous catalytic materials derived from metal-organic framework supports/precursors, Coord. Chem. Rev. 337 (2017) 80–96.

[101] Y.-Z. Chen, R. Zhang, L. Jiao, H.-L. Jiang, Metal–organic framework-derived porous materials for catalysis, Coord. Chem. Rev. 362 (2018) 1–23.

[102] B.N. Bhadra, A. Vinu, C. Serre, S.H. Jhung, MOF-derived carbonaceous materials enriched with nitrogen: preparation and applications in adsorption and catalysis, Mater. Today 25 (2019) 88–111.

[103] I. Ahmed, S.H. Jhung, Applications of metal-organic frameworks in adsorption/separation processes via hydrogen bonding interactions, Chem. Eng. J. 310 (2017) 197–215.

[104] S.-N. Kim, J. Kim, H.-Y. Kim, H.-Y. Cho, W.-S. Ahn, Adsorption/catalytic properties of MIL-125 and NH₂-MIL-125, Catal. Today 204 (2013) 85–93.

[105] T.W. Kim, M.J. Kim, F. Kleitz, M.M. Nair, R. Guillet-Nicolas, K.E. Jeong, H.J. Chae, C.U. Kim, S.Y. Jeong, Tailor-made mesoporous Ti-SBA-15 catalysts for oxidative desulfurization of refractory aromatic sulfur compounds in transport fuel, ChemCatChem 4 (2012) 687–697.

[106] N.D. McNamara, G.T. Neumann, E.T. Masko, J.A. Urban, J.C. Hicks, Catalytic performance and stability of (V) MIL-47 and (Ti) MIL-125 in the oxidative desulfurization of heterocyclic aromatic sulfur compounds, J. Catal. 305 (2013) 217–226.

[107] M. Dan-Hardi, C. Serre, T. Frot, L. Rozes, G. Maurin, C. Sanchez, G. Férey, A new photoactive crystalline highly porous titanium (IV) dicarboxylate, J. Am. Chem. Soc. 131 (2009) 10857–10859.

[108] K. Leus, I. Muylaert, M. Vandichel, G.B. Marin, M. Waroquier, V. Van Speybroeck, P. Van Der Voort, The remarkable catalytic activity of the saturated metal organic framework V-MIL-47 in the cyclohexene oxidation, Chem. Commun. 46 (2010) 5085–5087.

[109] N.D. McNamara, J.C. Hicks, Chelating agent-free, vapor-assisted crystallization method to synthesize hierarchical microporous/mesoporous MIL-125 (Ti), ACS Appl. Mater. Interfaces 7 (2015) 5338–5346.

[110] I.D. Ivanchikova, J.S. Lee, N.V. Maksimchuk, A.N. Shmakov, Y.A. Chesalov, A.B. Ayupov, Y.K. Hwang, C.-H. Jun, J.-S. Chang, O.A. Kholdeeva, Highly selective H₂O₂-based oxidation of alkylphenols to p-benzoquinones over MIL-125 metal-organic frameworks, Eur. J. Inorg. Chem. 2014 (2014) 132–139.

[111] Y. Zhang, G. Li, L. Kong, H. Lu, Deep oxidative desulfurization catalyzed by Ti-based metal-organic frameworks, Fuel 219 (2018) 103–110.

[112] G. Ye, Y. Sun, D. Zhang, W. Zhou, C. Lancelot, A. Rives, C. Lamonier, W. Xu, Hierarchical porous titanium terephthalate based material with highly active sites for deep oxidative desulfurization, Microporous Mesoporous Mater. 270 (2018) 241–247.

[113] M.Y. Masoomi, M. Bagheri, A. Morsali, Application of two cobalt-based metal–organic frameworks as oxidative desulfurization catalysts, Inorg. Chem. 54 (2015) 11269–11275.

[114] R. Abazari, S. Sanati, A. Morsali, A.M. Slawin, C.L. Carpenter-Warren, A dual-purpose 3D pillared metal–organic framework with excellent properties for catalysis of oxidative desulfurization and energy storage in asymmetric

[115] A. Gómez-Paricio, A. Santiago-Portillo, S. Navalón, P. Concepción, M. Alvaro, H. Garcia, MIL-101 promotes the efficient aerobic oxidative desulfurization of dibenzothiophenes, Green Chem. 18 (2016) 508–515.

[116] J.W. Yoon, Y.K. Seo, Y.K. Hwang, J.S. Chang, H. Leclerc, S. Wuttke, P. Bazin, A. Vimont, M. Daturi, E. Bloch, P.L. Llewellyn, C. Serre, P. Horcajada, J.-M. Grenèche, A.E. Rodrigues, G. Férey, Controlled reducibility of a metal–organic framework with coordinatively unsaturated sites for preferential gas sorption, Angew. Chem. Int. Ed. 49 (2010) 5949–5952.

[117] X. Zhang, P. Huang, A. Liu, M. Zhu, A metal–organic framework for oxidative desulfurization: UIO-66(Zr) as a catalyst, Fuel 209 (2017) 417–423.

[118] H.-Q. Zheng, Y.-N. Zeng, J. Chen, R.-G. Lin, W.-E. Zhuang, R. Cao, Z.-J. Lin, Zr-based metal–organic frameworks with intrinsic peroxidase-like activity for ultra-deep oxidative desulfurization: mechanism of H₂O₂ decomposition, Inorg. Chem. 59 (2019) 6983–6992.

[119] C. Piscopo, L. Voellinger, M. Schwarzer, A. Polyzoidis, D. Bošković, S. Loebbecke, Continuous flow desulfurization of a model fuel catalysed by titanium functionalized UiO-66, ChemistrySelect 4 (2019) 2806–2809.

[120] G. Ye, H. Qi, X. Li, K. Leng, Y. Sun, W. Xu, Enhancement of oxidative desulfurization performance over UiO-66 (Zr) by titanium ion exchange, ChemPhysChem 18 (2017) 1903–1908.

[121] C.M. Granadeiro, S.O. Ribeiro, M. Karmaoui, R. Valença, J.C. Ribeiro, B. de Castro, L. Cunha-Silva, S.S. Balula, Production of ultra-deep sulfur-free diesels using a sustainable catalytic system based on UiO-66(Zr), Chem. Commun. 51 (2015) 13818–13821.

[122] G. Ye, D. Zhang, X. Li, K. Leng, W. Zhang, J. Ma, Y. Sun, W. Xu, S. Ma, Boosting catalytic performance of metal–organic framework by increasing the defects via a facile and green approach, ACS Appl. Mater. Interfaces 9 (2017) 34937–34943.

[123] W. Xiao, Q. Dong, Y. Wang, Y. Li, S. Deng, N. Zhang, Time modulation of defects in UiO-66 and application in oxidative desulfurization, CrystEngComm 20 (2018) 5658–5662.

[124] G. Fu, B. Bueken, D. De Vos, MOF satalysts: Zr-metal-organic framework catalysts for oxidative desulfurization and their improvement by postsynthetic ligand exchange, Small Methods 2 (2018) 1800059.

[125] W. Trakarnpruk, K. Rujiraworawut, Oxidative desulfurization of Gas oil by polyoxometalates catalysts, Fuel Process. Technol. 90 (2009) 411–414.

[126] Y. Ding, W. Zhu, H. Li, W. Jiang, M. Zhang, Y. Duan, Y. Chang, Catalytic oxidative desulfurization with a hexatungstate/aqueous H₂O₂/ionic liquid emulsion system, Green Chem. 13 (2011) 1210–1216.

[127] J. Xu, S. Zhao, W. Chen, M. Wang, Y.-F. Song, Highly efficient extraction and oxidative desulfurization system using Na₇H₂LaW₁₀O₃₆·32 H₂O in [bmim]BF₄ at room temperature, Chem. Eur. J. 18 (2012) 4775–4781.

[128] C. Yansheng, L. Changping, J. Qingzhu, L. Qingshan, Y. Peifang, L. Xiumei, U. Welz-Biermann, Desulfurization by oxidation combined with extraction using acidic room-temperature ionic liquids, Green Chem. 13 (2011) 1224–1229.

[129] W. Zhu, W. Huang, H. Li, M. Zhang, W. Jiang, G. Chen, C. Han, Polyoxometalate-based ionic liquids as catalysts for deep desulfurization of fuels, Fuel Process. Technol. 92 (2011) 1842–1848.

[130] H. Ilbeygi, I.Y. Kim, M.G. Kim, W. Cha, P.S.M. Kumar, D.-H. Park, A. Vinu, Highly crystalline mesoporous phosphotungstic acid: a promising material for energy storage applications, Angew. Chem. Int. Ed. (2019).

[131] D.-Y. Du, J.-S. Qin, S.-L. Li, Z.-M. Su, Y.-Q. Lan, Recent advances in porous polyoxometalate-based metal–organic framework materials, Chem. Soc. Rev. 43 (2014) 4615–4632.

[132] C. Freire, D.M. Fernandes, M. Nunes, V.K. Abdelkader, POM & MOF-based electrocatalysts for energy-related reactions, ChemCatChem 10 (2018) 1703–1730.

[133] K. Fujie, H. Kitagawa, Ionic liquid transported into metal–organic frameworks, Coord. Chem. Rev. 307 (2016) 382–390.

[134] L. Chen, R. Luque, Y. Li, Controllable design of tunable nanostructures inside metal–organic frameworks, Chem. Soc. Rev. 46 (2017) 4614–4630.

[135] F.P. Kinik, A. Uzun, S. Keskin, Ionic liquid/metal–organic framework composites: from synthesis to applications, ChemSusChem 10 (2017) 2842–2863.

[136] N.A. Khan, B.N. Bhadra, S.H. Jhung, Heteropoly acid-loaded ionic liquid@metal-organic frameworks: effective and reusable adsorbents for the desulfurization of a liquid model fuel, Chem. Eng. J. 334 (2018) 2215–2221.

[137] I. Ahmed, T. Panja, N.A. Khan, M. Sarker, J.-S. Yu, S.H. Jhung, Nitrogen-doped porous carbons from ionic liquids@MOF: remarkable adsorbents for both aqueous and nonaqueous media, ACS Appl. Mater. Interfaces 9 (2017) 10276–10285.

[138] N.A. Khan, Z. Hasan, S.H. Jhung, Ionic liquid@MIL-101 prepared via the ship-in-bottle technique: remarkable adsorbents for the removal of benzothiophene from liquid fuel, Chem. Commun. 52 (2016) 2561–2564.

[139] N.A. Khan, Z. Hasan, S.H. Jhung, Ionic liquids supported on metal-organic frameworks: remarkable adsorbents for adsorptive desulfurization, Chem. Eur. J. 20 (2014) 376–380.

[140] G. Férey, C. Mellot-Draznieks, C. Serre, F. Millange, J. Dutour, S. Surblé, I. Margiolaki, A chromium terephthalate-based solid with unusually large pore volumes and surface area, Science 309 (2005) 2040–2042.

[141] X. Hu, Y. Lu, F. Dai, C. Liu, Y. Liu, Host–guest synthesis and encapsulation of phosphotungstic acid in MIL-101 via "bottle around ship": an effective catalyst for oxidative desulfurization, Microporous Mesoporous Mater. 170 (2013) 36–44.

[142] S. Ribeiro, A.D.S. Barbosa, A.C. Gomes, M. Pillinger, I.S. Gonçalves, L. Cunha-Silva, S.S. Balula, Catalytic oxidative desulfurization systems based on Keggin phosphotungstate and metal-organic framework MIL-101, Fuel Process. Technol. 116 (2013) 350–357.

[143] X.-S. Wang, Y.-B. Huang, Z.-J. Lin, R. Cao, Phosphotungstic acid encapsulated in the mesocages of amine-functionalized metal–organic frameworks for catalytic

oxidative desulfurization, Dalton Trans. 43 (2014) 11950–11958.

[144] L. Zhang, S. Wu, Y. Liu, F. Wang, X. Han, H. Shang, Immobilization of phospho-tungstic acid in an amino-containing metal–organic framework for oxidative de-sulfurization, Appl. Organomet. Chem. 30 (2016) 684–690.

[145] M. Sun, W.-C. Chen, L. Zhao, X.-L. Wang, Z.-M. Su, A PTA@MIL-101(Cr)-diatomite composite as catalyst for efficient oxidative desulfurization, Inorg. Chem. Commun. 87 (2018) 30–35.

[146] X.L. Hao, Y.Y. Ma, H.Y. Zang, Y.H. Wang, Y.G. Li, E.B. Wang, A poly-oxometalate-encapsulating cationic metal–organic framework as a heterogeneous catalyst for desulfurization, Chem. Eur. J. 21 (2015) 3778–3784.

[147] E. Rafiee, N. Nobakht, Keggin type heteropoly acid, encapsulated in metal-organic framework: a heterogeneous and recyclable nanocatalyst for selective oxidation of sulfides and deep desulfurization of model fuels, J. Mol. Catal. A Chem. 398 (2015) 17–25.

[148] Y.-L. Peng, J. Liu, H.-F. Zhang, D. Luo, D. Li, A size-matched POM@MOF com-posite catalyst for highly efficient and recyclable ultra-deep oxidative fuel de-sulfurization, Inorg. Chem. Front. 5 (2018) 1563–1569.

[149] X.-M. Zhang, Z. Zhang, B. Zhang, X. Yang, X. Chang, Z. Zhou, D.-H. Wang, M.-H. Zhang, X.-H. Bu, Synergistic effect of Zr-MOF on phosphomolybdic acid pro-motes efficient oxidative desulfurization, Appl. Catal. B 256 (2019), https://doi.org/10.1016/j.apcatb.2019.117804 117804.

[150] Z.-J. Lin, H.-Q. Zheng, J. Chen, W.-E. Zhuang, Y.-X. Lin, J.-W. Su, Y.-B. Huang, R. Cao, Encapsulation of phosphotungstic acid into metal–organic frameworks with tunable window sizes: Screening of PTA@ MOF catalysts for efficient oxi-dative desulfurization, Inorg. Chem. 57 (2018) 13009–13019.

[151] X.-S. Wang, L. Li, J. Liang, Y.-B. Huang, R. Cao, Boosting oxidative desulfurization of model and real gasoline over phosphotungstic acid encapsulated in metal–or-ganic frameworks: the window size matters, ChemCatChem 9 (2017) 971–979.

[152] Y. Liu, S. Liu, S. Liu, D. Liang, S. Li, Q. Tang, X. Wang, J. Miao, Z. Shi, Z. Zheng, Facile synthesis of a nanocrystalline metal–organic framework impregnated with a phosphovanadomolybdate and its remarkable catalytic performance in ultradeep oxidative desulfurization, ChemCatChem 5 (2013) 3086–3091.

[153] F. Yu, R. Wang, Deep oxidative desulfurization of dibenzothiophene in simulated oil and real diesel using heteropolyanion-substituted hydrotalcite-like compounds as catalysts, Molecules 18 (2013) 13691–13704.

[154] S. Otsuki, T. Nonaka, N. Takashima, W.H. Qian, A. Ishihara, T. Imai, T. Kabe, Oxidative desulfurization of light gas oil and vacuum gas oil by oxidation and solvent extraction, Energy Fuels 14 (2000) 1232–1239.

[155] K.-Y.A. Lin, H.-A. Chang, B.-J. Chen, Multi-functional MOF-derived magnetic carbon sponge, J. Mater. Chem. A 4 (2016) 13611–13625.

[156] B.N. Bhadra, I. Ahmed, S. Kim, S.H. Jhung, Adsorptive removal of ibuprofen and diclofenac from water using metal-organic framework-derived porous carbon, Chem. Eng. J. 314 (2017) 50–58.

[157] B.N. Bhadra, S.H. Jhung, A remarkable adsorbent for removal of contaminants of emerging concern from water: porous carbon derived from metal azolate frame-work-6, J. Hazard. Mater. 340 (2017) 179–188.

[158] B.N. Bhadra, J.Y. Song, S.-K. Lee, Y.K. Hwang, S.H. Jhung, Adsorptive removal of aromatic hydrocarbons from water over metal azolate framework-6-derived car-bons, J. Hazard. Mater. 344 (2018) 1069–1077.

[159] I. Ahmed, B.N. Bhadra, H.J. Lee, S.H. Jhung, Metal-organic framework-derived carbons: preparation from ZIF-8 and application in the adsorptive removal of sulfamethoxazole from water, Catal. Today 301 (2018) 90–97.

[160] B.N. Bhadra, J.K. Lee, C.-W. Cho, S.H. Jhung, Remarkably efficient adsorbent for the removal of bisphenol A from water: Bio-MOF-1-derived porous carbon, Chem. Eng. J. 343 (2018) 225–234.

[161] J.Y. Song, B.N. Bhadra, N.A. Khan, S.H. Jhung, Adsorptive removal of artificial sweeteners from water using porous carbons derived from metal azolate frame-work-6, Microporous Mesoporous Mater. 260 (2018) 1–8.

[162] H.J. An, B.N. Bhadra, N.A. Khan, S.H. Jhung, Adsorptive removal of wide range of pharmaceutical and personal care products from water by using metal azolate framework-6-derived porous carbon, Chem. Eng. J. 343 (2018) 447–454.

[163] B.N. Bhadra, S.H. Jhung, Adsorptive removal of wide range of pharmaceuticals and personal care products from water using bio-MOF-1 derived porous carbon, Microporous Mesoporous Mater. 270 (2018) 102–108.

[164] S. Joseph, D.M. Kempaiah, M. Benzigar, A.V. Baskar, S.N. Talapaneni, S.H. Jhung, D.-H. Park, A. Vinu, Metal organic framework derived mesoporous carbon nitrides with a high specific surface area and chromium oxide nanoparticles for CO$_2$ and hydrogen adsorption, J. Mater. Chem. A 5 (2017) 21542–21549.

[165] J. Kim, N.D. McNamara, T.H. Her, J.C. Hicks, Carbothermal reduction of Ti-modified IRMOF-3: an adaptable synthetic method to support catalytic nano-particles on carbon, ACS Appl. Mater. Interfaces 5 (2013) 11479–11487.

[166] J. Kim, N.D. McNamara, J.C. Hicks, Catalytic activity and stability of carbon supported V oxides and carbides synthesized via pyrolysis of MIL-47 (V), Appl. Catal. A 517 (2016) 141–150.

[167] B.N. Bhadra, J.Y. Song, N.A. Khan, S.H. Jhung, TiO$_2$-containing carbon derived from a metal-organic framework composite: a highly active catalyst for oxidative

desulfurization, ACS Appl. Mater. Interfaces 9 (2017) 31192–31202.

[168] N.D. McNamara, J. Kim, J.C. Hicks, Controlling the pyrolysis conditions of mi-croporous/mesoporous MIL-125 to synthesize porous, carbon-supported Ti cata-lysts with targeted Ti phases for the oxidation of dibenzothiophene, Energy Fuels 30 (2016) 594–602.

[169] Y. Zi, Z.J. Cai, S.Y. Wang, S.J. Ji, Synthesis of isatins by I$_2$/TBHP mediated oxi-dation of indoles, Org. Lett. 16 (2014) 3094–3097.

[170] M.A. Nunes, P.A. Mello, C.A. Bizzi, L.O. Diehl, E.M. Moreira, W.F. Souza, E.C. Gaudino, G. Cravotto, E.M. Flores, Evaluation of nitrogen effect on ultra-sound-assisted oxidative desulfurization process, Fuel Process. Technol. 126 (2014) 521–527.

[171] R.A. Sheldon, J.K. Kochi, Metal-catalyzed Oxidations of Organic Compounds: Mechanistic Principles and Synthetic Methodology Including Biochemical Processes, Academic Press, New York, 1981, pp. 18–68.

[172] F.S. Mjalli, O.U. Ahmed, T. Al-Wahaibi, Y. Al-Wahaibi, I.M. AlNashef, Deep oxi-dative desulfurization of liquid fuels, Rev. Chem. Eng. 30 (2014) 337–378.

[173] E. Lorençon, D.C. Alves, K. Krambrock, E.S. Ávila, R.R. Resende, A.S. Ferlauto, R.M. Lago, Oxidative desulfurization of dibenzothiophene over titanate nano-tubes, Fuel 132 (2014) 53–61.

[174] S.-x. Lu, H. Zhong, D.-m. Mo, Z. Hu, H.-l. Zhou, Y. Yao, A H-titanate nanotube with superior oxidative desulfurization selectivity, Green Chem. 19 (2017) 1371–1377.

[175] H. Wang, R. Zhou, Y. Deng, Thiophene oxidation with H$_2$O$_2$ over defect and perfect titanium silicalite-1: a computational study, React. Kinet. Mech. Catal. (2018) 1–16.

[176] N. Alonso-Fagúndez, M. Ojeda, R. Mariscal, J. Fierro, M.L. Granados, Gas phase oxidation of furfural to maleic anhydride on V$_2$O$_5$/γ-Al$_2$O$_3$ catalysts: reaction conditions to slow down the deactivation, J. Catal. 348 (2017) 265–275.

[177] C. Carrero, R. Schlögl, I. Wachs, R. Schomaecker, Critical literature review of the kinetics for the oxidative dehydrogenation of propane over well-defined supported vanadium oxide catalysts, ACS Catal. 4 (2014) 3357–3380.

[178] B.M. Reddy, S.-C. Lee, D.-S. Han, S.-E. Park, Utilization of carbon dioxide as soft oxidant for oxydehydrogenation of ethylbenzene to styrene over V$_2$O$_5$–CeO$_2$/TiO$_2$–ZrO$_2$ catalyst, Appl. Catal. B 87 (2009) 230–238.

[179] J. Kim, N.D. McNamara, J.C. Hicks, Catalytic activity and stability of carbon supported V oxides and carbides synthesized via pyrolysis of MIL-47(V), Appl. Catal. A 517 (2016) 141–150.

[180] H. Gómez-Bernal, L. Cedeño-Caero, A. Gutiérrez-Alejandre, Liquid phase oxidation of dibenzothiophene with alumina-supported vanadium oxide catalysts: an alter-native to deep desulfurization of diesel, Catal. Today 142 (2009) 227–233.

[181] M. Carraro, N. Nsouli, H. Oelrich, A. Sartorel, A. Sorarù, S.S. Mal, G. Scorrano, L. Walder, U. Kortz, M. Bonchio, Reactive Zr^{IV} and Hf^{IV} butterfly peroxides on polyoxometalate surfaces: bridging the gap between homogeneous and hetero-geneous catalysis, Chem. Eur. J. 17 (2011) 8371–8378.

[182] F. Faccioli, M. Bauer, D. Pedron, A. Sorarù, M. Carraro, S. Gross, Hydrolytic sta-bility and hydrogen peroxide activation of zirconium-based oxoclusters, Eur. J. Inorg. Chem. 2015 (2015) 210–225.

[183] M. Tarafder, M.L. Miah, Novel peroxo complexes of zirconium containing organic ligands, Inorg. Chem. 25 (1986) 2265–2268.

[184] A. Santiago-Portillo, S. Navalón, F.G. Cirujano, F.X.Lsi. Xamena, M. Alvaro, H. Garcia, MIL-101 as reusable solid catalyst for autoxidation of benzylic hydro-carbons in the absence of additional oxidizing reagents, ACS Catal. 5 (2015) 3216–3224.

[185] J. Kim, S. Bhattacharjee, K.-E. Jeong, S.-Y. Jeong, W.-S. Ahn, Selective oxidation of tetralin over a chromium terephthalate metal organic framework, MIL-101, Chem. Commun. (2009) 3904–3906.

[186] L.S. Nogueira, S. Ribeiro, C.M. Granadeiro, E. Pereira, G. Feio, L. Cunha-Silva, S.S. Balula, Novel polyoxometalate silica nano-sized spheres: efficient catalysts for olefin oxidation and the deep desulfurization process, Dalton Trans. 43 (2014) 9518–9528.

[187] C.N. Dai, J. Zhang, C.P. Huang, Z.G. Lei, Ionic liquids in selective oxidation: Catalysts and solvents, Chem. Rev. 117 (2017) 6929–6983.

[188] P.S. Kulkarni, C.A.M. Afonso, Deep desulfurization of diesel fuel using ionic li-quids: current status and future challenges, Green Chem. 12 (2010) 1139–1149.

[189] Z. Ismagilov, S. Yashnik, M. Kerzhentsev, V. Parmon, A. Bourane, F. Al-Shahrani, A. Hajji, O. Koseoglu, Oxidative desulfurization of hydrocarbon fuels, Catal. Rev. Sci. Eng. 53 (2011) 199–255.

[190] A. Bazyari, A.A. Khodadadi, A.H. Mamaghani, J. Beheshtian, L.T. Thompson, Y. Mortazavi, Microporous titania–silica nanocomposite catalyst-adsorbent for ultra-deep oxidative desulfurization, Appl. Catal. B 180 (2016) 65–77.

[191] J.M. Fraile, C. Gil, J.A. Mayoral, B. Muel, L. Roldán, E. Vispe, S. Calderón, F. Puente, Heterogeneous titanium catalysts for oxidation of dibenzothiophene in hydrocarbon solutions with hydrogen peroxide: on the road to oxidative de-sulfurization, Appl. Catal. B 180 (2016) 680–686.

[192] N. Montoya Sánchez, A. de Klerk, Autoxidation of aromatics, Appl. Petrochem. Res. 8 (2018) 55–78.